10-22-2019 9:30 AM

Effect of N-acetyl-L-cysteine prevention or intervention on diet induced beta cell compensation and dysfunction

Madison Wallace, *The University of Western Ontario*

Supervisor: Wang, Rennian, *The University of Western Ontario, Children's Health Research Institute*

A thesis submitted in partial fulfillment of the requirements for the Master of Science degree in Pathology and Laboratory Medicine

Abstract

Type 2 diabetes mellitus (T2DM) progression increases oxidative stress which contributes to beta cell compensation and eventual dysfunction. To investigate the role of antioxidant N-acetyl-L-cysteine (NAC) on beta cell function and pancreatic stellate cell activation (αSMA^+) during early and late stages of compensation, NAC was used for preventative (p) and intervention (i) treatments in C57BL/6N mice fed a 60% kcal high-fat diet (HFD) for 8 or 22 weeks. Significantly improved glucose tolerance was observed at 22 weeks following pNAC treatment in HFD mice. Although 22-week HFD mice displayed hyperinsulinemia, beta cell hypertrophy, decreased beta cell PDX-1 nuclear localization, and increased intra-islet αSMA^+ cells, HFD mice with iNAC treatment normalized beta cell mass and insulin secretion, improved nuclear PDX-1 labeling, and decreased intra- islet αSMA^+ staining. In conclusion, NAC treatment prevented beta cell over-compensation associated dysfunction and improved metabolic outcomes in diet-induced obesity T2DM mouse models.

Keywords: Type 2 diabetes, oxidative stress, beta cell, N-acetyl-L-cysteine, pancreatic stellate cell, high-fat diet

Summary for Lay Audience

Type 2 diabetes mellitus (T2DM) is a progressive disease that occurs in multiple stages, with each stage causing increased levels of stress on cells responsible for lowering blood sugar through the hormone insulin. Early in T2DM, the body requires more insulin production. Insulin-producing cells can keep up with this demand for a short period of time by increasing their size and number. However, the increased demand for insulin causes insulin-producing cells to develop complications, which eventually leads to their failure. The drug N-acetyl-L-cysteine (NAC) has been shown to decrease a type of stress found in T2DM insulin-producing cells. This study determined whether decreasing the stress using NAC could help protect the insulin-producing cells, and when it was most effective. When NAC was given to mice that demonstrated T2DM progression, their insulin-producing cells were partially protected from developing dysfunction when compared to insulin-producing cells from T2DM mice not treated with NAC. These cells increased markers of their ability to produce and release insulin, did not increase in size, and did not overproduce insulin, suggesting they were functioning more like the normal insulin-producing cells rather than those experiencing T2DM. However, no significant improvement was found in overall blood sugar levels from T2DM mice treated with NAC. When NAC was given to mice one week before T2DM started, significant improvements in blood sugar levels and improvements in the size of the insulin-producing cell area were found. In conclusion, NAC may be able to protect insulin-producing cells from the dysfunction associated with overcompensation during T2DM, as well as whole-body metabolic changes when taken early enough and for a long-time duration.

Co-Authorship Statement

The methodology described in Chapter 2 was conducted primarily by Madison Wallace in the lab of Dr. Rennian Wang. Members in the lab made the following contributions:

Dr. Amanda Oakie provide technical assistance with immunofluorescence staining, imaging, and metabolic testing. Dr. Amanda Oakie also provided insight and guidance, along with assistance during thesis editing and organization. Gurleen Sahi conducted beta cell mass analysis for the 22-week prevention NAC study in figure 3.12a and b. Studies were designed by Dr. Rennian Wang. Dr. Wang also provided insight into data interpretation and organization, assistance with figure organization, and revisions to this thesis.

Acknowledgments

I would like to thank Dr. Rennian Wang for giving me the chance to pursue a master's degree in her lab. You provided an opportunity to learn and grow both personally and professionally and I appreciate your mentorship more than I can express. I plan to carry the lessons you have taught me through each of the following chapters of my life. I would also like to thank Dr. Amanda Oakie; you have been an amazing peer mentor and friend during my time here, providing expertise and encouragement every step of the way. Thank you to all past and current members of the Wang lab for your role in creating a positive experience during my time here.

Thank you to my advisory committee members, Dr. Nica Borradaile and Dr. Chandan Chakraborty for your guidance. I truly appreciate your insights during my project as well as your assistance in editing the chapters of this thesis. A special thanks to the members of Dr. Cindy Hutnik's lab, who have shown me kindness and support throughout my time in the department.

Finally, I would like to thank my friends and family. To everyone I have been lucky to call a friend: I truly appreciate all the kind words, useful advice, and great memories you have given me. To my parents: thank you for all your love and guidance, as well as for lifting me up any time I needed courage or strength. To my brothers: thank you for always being a shoulder for me to lean on when I needed to talk, and for being such incredible examples of hard work and perseverance. To my Grampy and Mar: thank you for taking me in when I needed somewhere to stay, for always lending an ear on a hard day, and for the home cooked food. To my Poppa: thank you for always being only a phone-call away, and for offering wisdom and support throughout my high and low points.

The project within this thesis was funded by the Canadian Institutes of Health Research (CIHR).

Table of Contents

List of Tables

List of Figures

List of Appendices

List of Abbreviations

aSMA	alpha-SMA
AUC	Area under the curve
B6J	C57BL6/J mouse strain
B6N	C57BL/6N mouse strain
DAPI	4′,6-diamidino-2-phenylindole
DIO	Diet induced obesity
DPP-4	dipeptidyl peptidase 4
ECM	Extra-cellular matrix
ELISA	Enzyme-linked immunosorbent assay
GK	Goto-Kakizaki Rat
GSH	Glutathione
GSSG	Glutathione disulfide
HFD	High-fat diet
HFD+iNAC	High-fat diet with NAC intervention treatment
HFD+pNAC	High-fat diet with NAC prevention treatment
FITC	Fluorescein isothiocyanate
FBG	Fasting blood glucose
IF	Immunofluorescence
IPITT	Intra-peritoneal insulin tolerance test

IPGTT	Intra-peritoneal glucose tolerance test
MMP	Matrix metalloproteinase
NAC	N-acetyl-L-cysteine
NADPH	nicotinamide adenine dinucleotide phosphate hydrogen
ND	Normal diet
ND+iNAC	Normal diet with NAC intervention treatment
ND+pNAC	Normal diet with NAC prevention treatment
NNT	nicotinamide nucleotide transhydrogenase
PaSC	Pancreatic stellate cell
PBS	Phosphate buffered saline
PDX-1	Pancreatic and duodenal homeobox 1
ROS	Reactive oxygen species
SEM	Standard error of the mean
SNARE	Soluble N–ethylmaleimide sensitive factor (NSF) attachment protein receptor
STZ	Streptozotocin
TIMP	Tissue inhibitor of matrix metalloproteinases
T1DM	Type 1 diabetes mellitus
T2DM	Type 2 diabetes mellitus
TRITC	tetramethyl rhodamine isothiocyanate

Chapter 1

1 Introduction

1.1 Significance of the Study

Type 2 diabetes mellitus (T2DM) is a complex disease with multiple stages of progression, involving intrinsic compensatory mechanisms as well as dysfunctional over-exertion of the beta cells. During the progression of T2DM, levels of oxidative stress increase and can cause direct damage to both islets and peripheral tissues. Short- and long-term antioxidant treatment of T2DM with N-acetyl-L-cysteine (NAC) has been found to reduce oxidative stress levels in peripheral tissue and improve insulin resistance and glucose tolerance in diet-induced obesity (DIO) rodent models of T2DM. However, short-term NAC administration has not demonstrated efficacy in diabetic patients. This has led to the hypothesis that NAC treatment efficacy may be dependent on the time-point and duration of its administration. While the effects of NAC on peripheral tissues have been extensively reported, its effects on beta cell function *in vivo* are still not well understood. This work examines the impact of NAC administration at different time points in a DIO rodent model on beta cell compensation and dysfunction.

1.2 Overview of the Pancreas and the Islets of Langerhans

Unlike the human pancreas, which has a defined shape, the rodent pancreas is a diffuse organ that stretches horizontally between the duodenum and spleen before continuing to the mesentery surrounding the duodenum (Dolenšek et al., 2015). The exocrine pancreas accounts for approximately 96% of total pancreas volume (Dolenšek et al., 2015) and is responsible for the production and secretion of digestive enzymes through the pancreatic duct to the duodenum (Campbell-Thompson, Rodriguez-Calvo, & Battaglia, 2015). The islets of Langerhans, which compose only 1-2% of the total pancreas volume, contain endocrine cells that produce multiple hormones involved in maintaining glucose homeostasis. There are five main cell types within the islets: alpha, beta, delta, gamma, and epsilon cells that produce glucagon, insulin, somatostatin, pancreatic polypeptide, and ghrelin, respectively (Campbell-Thompson et al., 2015). The most abundant

endocrine cell type in the rodent islet is the beta cell (60-80%), found within the core of the islet, followed by the alpha cells located on the periphery (10-20%). In contrast, human islets contain a more scattered distribution of beta and alpha cells throughout the islet, with a slightly lower beta to alpha cell ratio (Dolenšek et al., 2015).

1.3 Beta Cell Identity and Function

To properly respond to increased blood glucose levels, beta cells must maintain mature beta cell identity through active regulation of gene expression using transcription factors such as pancreatic and duodenal homeobox-1 (PDX-1). In beta cells, nuclear PDX-1 is involved in sensing and responding to high glucose environments by up-regulating insulin transcription (Ahlgren et al., 1998; Kaneto et al., 2015). Once the islets have reached maturity, beta cells have very low proliferation rates and an average mass of about 1 mg (Chintinne et al., 2012). Alterations in levels of transcription factors, proteins responsible for insulin release, proliferation rates, and beta cell mass can all be found during the progression of islet pathology during T2DM.

In response to a post-prandial blood glucose, the beta cells release insulin in two phases. Circulating glucose enters the beta cell and triggers membrane depolarization and an influx of Ca^{2+} ions, beginning release of insulin into the blood stream. During phase one of biphasic insulin release, insulin-containing vesicles that are pre-docked to the plasma membrane through SNARE protein complex formation between the vesical and the plasma membrane (Hou et al., 2009), the readily releasable pool of granules, undergo exocytosis. Following this short and rapid burst of insulin release, phase two insulin granules from the reserve pool translocate to the same plasma membrane release sites for exocytosis (Henquin et al., 2002). Insulin release allows for GLUT4-mediated glucose uptake into adipose tissue and skeletal muscle for energy use and storage (Rossmeisl et al., 2003) as well as suppresses liver metabolism of glycogen, allowing the body to return to normoglycemia (Hou et al., 2009; Straub & Sharp, 2002). While beta cells are known to respond during hyperglycemic conditions, under physiological conditions alpha cells respond to hypoglycemia by releasing glucagon in order to raise blood glucose levels. This results in stimulation of the liver to break down glycogen into glucose to maintain normoglycemia (Titchenell et al., 2017).

1.4 Diabetes Mellitus in Humans

The two major types of diabetes mellitus are distinguished based on the etiology that ultimately leads to beta cell failure. Type 1 diabetes mellitus (T1DM) is an autoimmune disorder where the body targets insulin-secreting beta cells and induces cell death, leading to insufficient insulin production (Kosiewicz et al., 2019). Due to the severity of beta cell loss, exogenous insulin is required to avoid hyperglycemia. T2DM is a multifactorial disease that progresses through a series of stages that include whole body and pancreatic alterations (Figure 1.1). Stage progression during T2DM in humans does not always occur in a strictly linear fashion, but typically begins with a shift from a metabolically healthy to a prediabetic state that is often facilitated by obesity (Keane et al., 2015; McAdam-Marx et al., 2014). The prediabetic state is characterized by hyperinsulinemia and insulin resistance in peripheral tissues (Yang et al., 2016), where insulin receptor signaling that allows glucose uptake and storage no longer properly responds to insulin signaling. Prediabetes includes a compensatory mechanism where beta cells increase insulin output to overcome reduced insulin receptor sensitivity and achieve normoglycemia (Butler et al., 2003; Prentki & Nolan, 2006). The progression to later stages of T2DM depends on multiple influences, including environmental and genetic factors. Glycemic control is no longer observed during full T2DM (Wu et al., 2014).

Early treatments for T2DM may include lifestyle changes, such as diet and exercise. In cases where medication is necessary, the most commonly prescribed treatments decrease liver gluconeogenesis and increase peripheral tissue glucose uptake (metformin) or increase beta cell insulin release (DPP-4 inhibitors or sulfonylureas). In severe cases of beta cell dysfunction, exogenous insulin may be required (Marín-Peñalver et al., 2016).

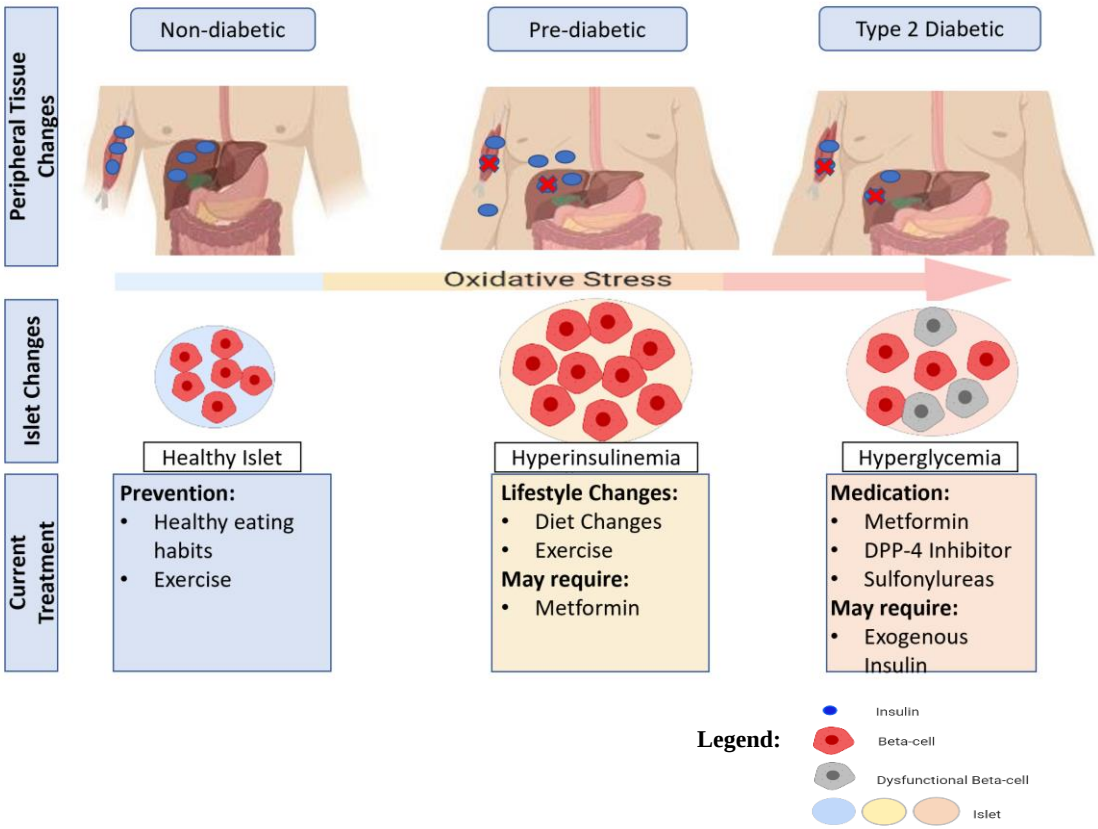

Figure 1.1: T2DM progression in peripheral tissue and islet morphology. In a non-diabetic individual, insulin binds to insulin receptor to allow for GLUT4 -regulated glucose uptake on skeletal muscle and adipose tissue and suppression of glycogen production in the liver. Islets at this time have unaltered beta cell activity and no intervention is required with the maintenance of healthy eating and lifestyle patterns. In the pre-diabetic stage of T2DM progression, oxidative stress levels increase due to insulin resistance. Due to the tissue's inability to respond to insulin, an increased demand is placed on the beta cells that then induces increased size and/or number, leading to hyperinsulinemic levels that are able to maintain normoglycemia. Treatment at this time-point includes improving diet and exercise but may progress to requiring metformin. In later stages of T2DM, the beta cells can no longer keep up with the high insulin demand and results in beta cell dysfunction and hyperglycemic conditions. Treatments of late-stage T2DM patients involves drugs such as metformin or sulfonylureas, but exogenous insulin may be required if beta cell dysfunction is extensive. Figure created with BioRender.

1.5 Diabetic Animal Models for T2DM Research

Diabetic animal models have played an important role in elucidating the specific nature of insulin regulation, secretory defects, and limitations of beta cell growth to provide a better understanding of T2DM and its associated complications. It has been found that high-fat diet (HFD) induced T2DM progression in C57 black 6 (C57BL/6) mice is similar to the progression found in humans as the C57BL/6J and C57BL/6N mouse lines are susceptible to HFD-induced weight gain, hyperinsulinemia, and hyperglycemia (Nicholson et al., 2010). In another rodent model of T2DM, the Sprague-Dawley rat, increased levels of systemic reactive oxygen species (ROS) accumulation caused by increased intake of free fatty acids (FFAs), lipid peroxidation, and decreased antioxidant status, lead to the development of oxidative stress (Zhang et al., 2010). As over nutrition and oxidative stress progress, the beta cell compartment is unable to maintain normal regulation and beta cell identity (Ježek et al., 2019). Beta cells in this stage begin compensatory measures to attempt to re-establish normoglycemia.

While C57BL/6J (B6J) is a very common strain used in DIO T2DM modelling, C57BL/6N (B6N) is also highly susceptible to 60% HFD and possess a slightly different genetic background and presentation of T2DM (Nicholson et al., 2010). B6N strain of mouse was derived from the same parent strain of C57BL/6 mice as B6J mice, however, B6N mice have been known to display a slightly milder phenotype of T2DM (Fontaine & Davis, 2016). Interestingly, while B6J mice display the more severe phenotype, reduced insulin secretion is found to be independent of changes in beta cell mass or insulin sensitivity in lean mice, suggesting an insulin secretion defect in the B6J sub strain likely related to the nicotinamide nucleotide transhydrogenase (*Nnt)* allele mutation found in B6J, but not B6N, mice (Aston-Mourney et al., 2007; Fergusson et al., 2014). The *Nnt* allele encodes a mitochondrial enzyme for Nnt, a part of a proton pump responsible for nicotinamide adenine dinucleotide phosphate hydrogen (NADPH) generation (Aston-Mourney et al., 2007). Possession of the wild-type *Nnt* allele may make the B6N strain more comparable to the human condition as it is present within human mitochondria (Fisher-Wellman et al., 2016). Additionally, less genetic variability has been found between mice of the B6N sub strain compared to B6J mice (Mekada et al., 2009), which

combined with the lack of potential compensatory mechanisms found in B6J mice associated with loss of Nnt function, has led to the suggestion that B6N mice may be a better representation of metabolic disorder (Fisher-Wellman et al., 2016).

1.6 Beta Cell Compensation in T2DM

As over-nutrition induces peripheral insulin resistance and impaired glucose tolerance (Rani et al., 2016), the beta cells respond to the increased insulin demand and stress signaling by initiating hypertrophy (Cox et al., 2016) and increasing proliferation rates (Mosser et al., 2015). These beta cells enter a compensatory phase of insulin secretion and display an increase in nuclear FOXO1 staining, which has been associated with increased insulin secretion (Zhang et al., 2016). However, while the increase in nuclear FOXO1 has been shown to be necessary for increased insulin release during metabolic stress, it can also induce beta cell dysfunction and reduced beta cell mass (Kobayashi et al., 2012). As beta cell compensation progresses towards dysfunction, they display reduced nuclear PDX-1 staining due to high levels of oxidative stress (Kawamori et al., 2003) In addition to the beta cell-specific changes, prolonged HFD-induced compensation affects the islet microenvironment by increasing collagen deposition and intra-islet pancreatic stellate cell activation (PaSC) (Lee et al., 2017). Eventually, the beta cells are no longer able to compensate and a decrease in functional beta cell mass is observed due to dysfunction and loss of mature beta cell identity related to chronic oxidative stress and glucotoxicity (Prentki & Nolan, 2006; Swisa et al., 2017).

1.7 Pancreatic Stellate Cells in T2DM

The PaSC is a mesenchymal-like cell type located throughout the periacinar regions of the pancreas and within the pancreatic islets (Zha et al.,2014), constituting about 4% of all pancreatic cells (Apte et al., 1998). The majority of PaSCs are quiescent under physiological conditions and are primarily responsible for extracellular matrix turnover via the balanced production of matrix metalloproteinases (MMPs) and tissue inhibitors of matrix metalloproteinases (TIMPS) (Xue et al., 2018). PaSC activation occurs with ROS accumulation, mechanical stress, or cytokine activation, causing these cells to take on a myofibroblast phenotype. Once active, PaSCs express alpha smooth muscle actin

(αSMA) and increase their production of collagen I, platelet derived growth factor, transforming growth factor beta, interleukin 1-beta, and various other inflammatory cytokines and fibrosing responses that can be harmful to the islets (Hayden et al., 2007; Masamune et al.,2009).

Active PaSCs have been identified as major contributors to fibrosis in the course of various pancreatic pathologies, including pancreatitis and pancreatic cancer, due to their dysfunctional MMP/TIMP balance and increased collagen deposition. They are also reported to play a role in up-regulating the epithelial-mesenchymal transition of pancreatic cancer cells, allowing for their increased ability to metastasize (Pandol & Edderkaoui, 2015). In addition to their support of tumor metastasis, PaSCs have been shown to promote inflammation within the islets, both through increased secretion of cytokines as well as interaction with inflammatory cells, promoting increased macrophage infiltration (Pandol & Edderkaoui, 2015; Saito et al., 2012).

Recent evidence has demonstrated that active PaSCs can contribute to factors involved in the progression of T2DM (Figure 1.2). Hyperinsulinemia and hyperglycemia are able to increase oxidative stress, contributing to beta cell dysfunction. It has been shown that high levels of insulin and glucose are also found to have both independent and additive effects on the activation and proliferation of PaSCs (Hong et al., 2007). The activation of PaSCs under hyperglycemic and hyperinsulinemic stresses were found to be related to increased levels of oxidative stress in PaSCs (Ryu et al., 2013). Active PaSCs are able to increase levels of insulin when co-cultured with beta cells for a short time period. However, due to a potential lack of insulin replenishment (Zang et al., 2015), co-culture contributes to long term beta cell dysfunction and decreased insulin response over multiple days, and is associated with beta cell dysfunction and apoptosis (Kikuta et al., 2013; Zang et al., 2015).

Due to negative impacts found following activation of PaSCs, methods of reducing PaSC activation have been investigated. When activated by the culture process due to mechanical stress and ROS accumulation, PaSCs can be returned to a quiescent phenotype using Matrigel as well as NAC (Jesnowski et al., 2005). Using plant alkaloid

conophylline to reduce intra-islet PaSC activation in Goto-Kakizaki (GK) rats, a reduction in islet fibrosis and an increase in pancreas insulin content were noted (Saito et al., 2012). However, whether a definitive relationship exists between PaSC activation and beta cell dysfunction has not yet been established (Lee et al., 2017), and whether short-term activation of PaSCs plays a role in increasing beta cell compensation has yet to be determined.

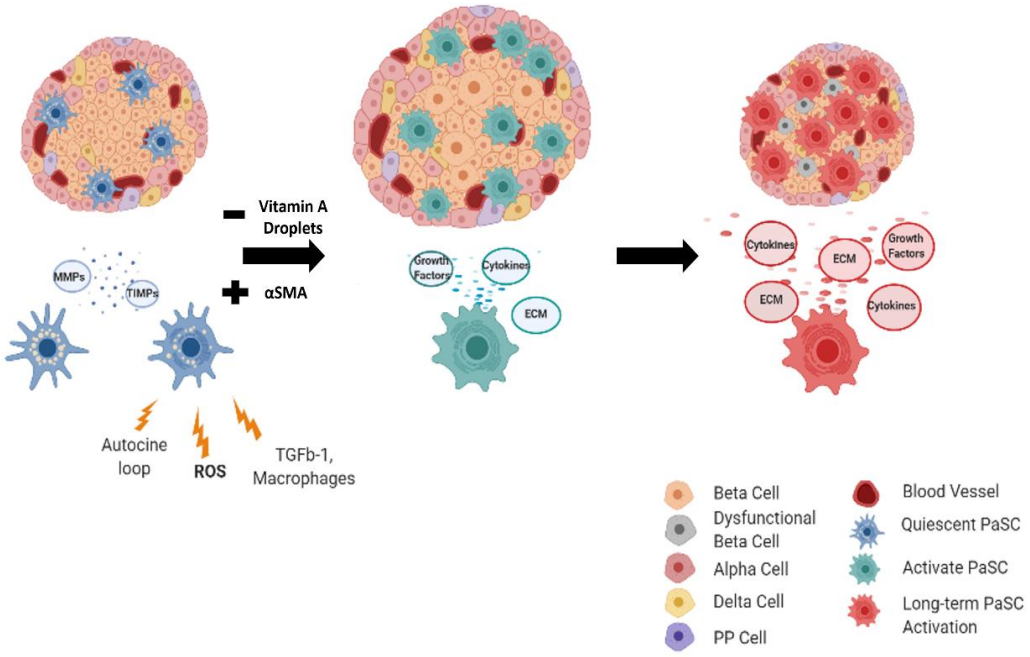

Figure 1.2: PaSC activation and proposed interaction with beta cells

PaSCs exist in the physiological islet in a quiescent state, where they primarily regulate ECM turnover through the production of MMPs and TIMPs. Following their activation, quiescent PaSCs lose their vitamin A droplets and become αSMA^{+} myofibroblast-like cells (left figure). Active PaSCs then produce growth factors, cytokines, and ECM components that may contribute to beta cell growth during compensation (middle figure). However, PaSCs are able to maintain long-term activation through autocrine and paracrine loops and could potentially become over-active, resulting in the over-production of ECM components and inflammatory cytokines (right figure). This over-production from PaSCs could lead to the islet fibrosis and inflammation found in T2DM and contribute to eventual beta cell dysfunction. Figure created with BioRender.

1.8 Oxidative Stress in T2DM

An imbalance between reactive oxygen species (ROS) and antioxidants in T2DM patients leads to an increase in oxidative stress. These ROS are mainly believed to be produced by the mitochondria in response to increased glucose and are normally reduced via intracellular antioxidants such as glutathione to a less harmful species (Sies, 2017). However, plasma samples from T2DM patients show increased lipid peroxides and reactive oxygen metabolites compared to non-diabetic controls, which is associated with significantly lower glutathione (GSH) levels (Sekhar et al., 2011). GSH is a tripeptide made up of glutamate, cysteine, and glycine, and functions as a major ROS scavenger in both human and rodent systems. While most mammalian cells can synthesize GSH, it is mainly produced and released by hepatocytes (Wu et al., 2004). Low GSH levels are caused by oxidation of GSH to become glutathione disulfide (GSSG) in conditions with increased levels of ROS, leading to a reduced GSH/GSSG ratio which cannot be naturally rectified through compensation with increased GSH synthesis, a problem commonly attributed to lack of precursor limited availability of precursors such as cysteine (Fujii et al., 2011; Sekhar et al., 2011). When deficient, GSH itself cannot be effectively replenished through oral administration due to the metabolic action of γ-glutamyltransferase, a transferase capable of hydrolyzing GSH in the intestine (Cohen et al., 1969; Springer-Verlag et al., 1992). Lack of GSH formation may be partially attributed to the low cysteine levels found in the blood of T2DM patients compared to non-diabetic controls. However, cysteine is non-polar and has poor intestinal absorption levels paired with rapid hepatic metabolism, making oral cysteine administration another poor option for increasing cysteine levels.

In order to increase cysteine and GSH levels, an acetyl group is added to cysteine to create NAC, most of which can be absorbed through the intestinal wall. Following oral ingestion and intestinal absorption, NAC undergoes extensive first pass metabolism by the liver that greatly reduces its bioavailability (Lasram et al., 2015). NAC deacetylates in the blood of the hepatic portal vein and L-cysteine enters the hepatocytes to become GSH (Tran et al., 2004). GSH is then able to function as a reactive oxygen species scavenger (Figure 1.2).

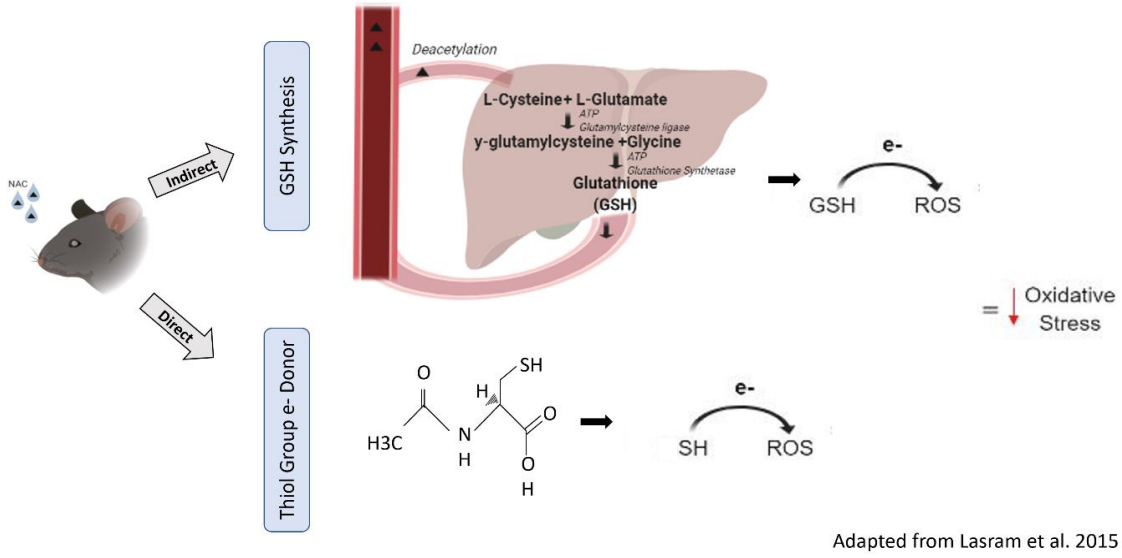

Figure 1.3: The direct and indirect mechanisms of NAC antioxidant action

Following intake through the drinking water, NAC is known to have either an indirect or direct mechanisms of antioxidant action. The indirect method is thought to be the predominant method, wherein NAC is deacetylated to become L-cysteine and proceeds to enter the liver. L-cysteine then binds to L-glutamate during an adenosine-triphosphate (ATP)-dependent reaction catalyzed by glutamyl cysteine ligase to become γ-glutamlycysteine. Glycine is then required to join γ-glutamlycysteine through another ATP-dependent reaction reliant on the glutathione synthetase enzyme to ultimately create GSH. GSH is then able to act as a ROS scavenger. Alternatively, NAC can act as a direct ROS scavenger due to the ability of its thiol group to donate electrons to reactive oxygen species. Figure created with BioRender.

1.9 Research on Antioxidant Therapies for T2DM

Due to the evidence of rising levels of oxidative stress and decreased levels of intrinsic antioxidants in T2DM patients, antioxidant therapies are often studied in T2DM research models. Various strategies have been attempted, including enzymatic antioxidants (Glutathione peroxidase mimetics), antioxidant vitamins (Vitamin C), and non-vitamin antioxidants (Coenzyme Q10, NAC) (Table 1.1) (Rochette et al., 2014). However, while antioxidants have been studied in various rodent models, NAC has shown efficacy in improving metabolic outcomes in DIO models of the disease, which closely resemble human progression of T2DM (Shen et al., 2019). NAC has also proven to be useful in improving insulin sensitivity in human patients with polycystic ovary syndrome (Dasgupta et al., 2015).

NAC is well known as a biosynthetic precursor to GSH, as the ability of NAC to increase levels of GSH is an indirect antioxidant effect and is reported to be its main mechanism of antioxidant action (Ma et al., 2016). However, NAC also contains a thiol group that can donate electrons to unstable ROS elements such as hydrogen peroxide, which then exerts direct antioxidant effects (Lasram et al., 2015). Due to its abilities as an antioxidant as well as a mucolytic agent, NAC is currently used in the clinical setting as a treatment or adjuvant treatment of various pathologies, some of which include acetaminophen overdose, chronic obstructive pulmonary disease, clomiphene citrate resistant polycystic ovary syndrome, chronic bronchitis, and liver cancer (Dekhuijzen, 2004; Lasram et al., 2015; Mokhtari et al., 2017).

NAC administration through drinking water has been shown to improve metabolic outcomes in DIO rodent models of T2DM. Specifically, improved glucose tolerance is found to be linked to increased insulin sensitivity following NAC administration. This increase in insulin sensitivity was associated with decreased fat accumulation in the liver (Falach-Malik et al., 2016) and decreased accumulation of visceral fat (Shen et al., 2019). While the decrease in fat accumulation was not found to be due to reduced caloric intake, which was unchanged in NAC treated rodents when compared to control litter-mates

(Falach-Malik et al., 2016; Novelli et al., 2009; Shen et al., 2019), this significant change in body weight may be connected to increased motor activity that enhances resting metabolic rates as well as fat oxidation (Novelli et al., 2009; Shen et al., 2019).

In vitro models of cultured islets treated with NAC have shown that the antioxidant is capable of reducing levels of oxidative stress, predominantly related to the presence of H_2O_2. When administered to pancreatic islets isolated from Wistar Rats and treated with dexamethasone, a corticosteroid associated with the ability to increase levels of oxidative stress related to increased levels of H_2O_2 (Roma et al., 2013; Tome et al., 2011), NAC was able to improve beta cell insulin release following stimulatory concentrations of glucose compared to islets treated with only dexamethasone (Roma et al., 2013). Additionally, it has been shown that increasing ribose levels in islets cultured from Wistar rats increased oxidative stress, which was improved by NAC administration. (Tanaka et al., 2002).

Table 1.1. Antioxidant subgroups used in models of T2DM

Drug Name, Type	Antioxidant Function	Efficacy in Rodent Model of T2DM	Efficacy in Human Study of T2DM
Ebselen, Glutathione Peroxidase Mimetic	Catalyzes reduction of H_2O_2 to H_2O	•Improve hyperinsulinemia, hyperglycemia, nuclear PDX-1 in beta cells, decrease beta cell apoptosis in Zucker diabetic fatty rat (Mahadevan et al., 2013)	•No improvement in levels of oxidative stress (Beckman et al., 2016)
Vitamin C, Antioxidant Vitamin	Electron Donor	•Mice able to compensate for vitamin C deficiency via hepatic *de novo* biosynthesis. Obesity linked to deficiency in humans. (Tranberg et al., 2014)	•May improve glucose concentration in T2DM patients with higher BMI's when administered for <30 days (Ashor et al., 2017)
Coenzyme Q10, Non-vitamin Antioxidant	Scavenge free lipid radicals, ROS in cellular membrane	•Prevent lipid accumulation in B6J DIO non-alcoholic fatty liver disease model (Frei et al., 1990; Chen et al., 2019)	•Improves glycemic control in patients with metabolic syndrome but not in T2DM patients (Suksomboon et al., 2015; Raygan et al., 2016)
NAC, Non-vitamin Antioxidant	Glutathione Precursor	•Improve hyperinsulinemia, hyperglycemia in DIO B6J mouse model (Falach-Malik et al., 2016; Shen et al., 2019)	•Lack of improvement on markers of glucose metabolism following short-term NAC treatment (Szkudlinska et al., 2016) •Improves insulin sensitivity in PCOS patients (Dasgupta et al., 2015)

1.10 Project Purpose and Outline

Previous research has demonstrated that NAC treatment in rodents improved glucose tolerance and insulin sensitivity, and that the efficacy of NAC to induce this improvement is dependent on the treatment dosage (Falach-Malik et al., 2016). NAC has also been shown to decrease levels of oxidative stress in pancreatic islets *in vitro* (Roma et al., 2013; Tanaka et al., 2002) and has been able to improve glucose tolerance in mice (Falach-Malik et al., 2016; Shen et al., 2019). However, clinical trials on T2DM patients have found that NAC treatments are not effective (Szkudlinska, Von Frankenberg, & Utzschneider, 2016). While NAC has demonstrated different levels of efficacy depending on length of administration, whether NAC is effective as a preventative treatment in short- or long-term studies has yet to be determined in rodents. In addition, no study to date has examined the effects of duration-dependent NAC treatments on beta cell function during the progression of T2DM. For this thesis, I studied the effects of NAC administration on glucose tolerance and beta cell compensation in a DIO mouse model during short-term (8 weeks) and long-term (22 weeks) prevention treatments as well as during NAC intervention (at 12 weeks of a 22-week HFD) treatment.

Objective:

To assess the effects of NAC on glucose tolerance and beta cell compensation when administered as a preventative or as an intervention treatment during HFD-induced T2DM progression in mice.

Hypothesis:

Prevention or intervention treatment using NAC during HFD-associated beta cell stress will improve glucose tolerance, beta cell function, and the expression of activated intra-islet (αSMA^{+}) PaSCs in mice.

Specific Questions:

1. What duration of HFD is required to induce glucose intolerance and insulin resistance?

2. Does administration of NAC prior to the beginning of HFD prevent glucose intolerance in mice?

3. Does preventative NAC administration enhance beta cell mass during early compensation in HFD mice?

4. Is preventative NAC treatment able to inhibit the intra-islet activation of PaSCs *in vivo*?

5. Does administration of NAC during HFD improve glucose tolerance in mice?

6. Does administration of NAC during HFD prevent later stage beta cell failure associated with T2DM progression?

7. Is intervention NAC treatment able to reduce PaSC activation during HFD *in vivo*?

Chapter 2

2 Research Design and Methods

2.1 Mouse colony maintenance and experimental design for NAC treatments

Male C57BL/6N (B6N) mice purchased from Charles River (Charles River Laboratories Quebec, Canada) were bred and housed in our facility with a maximum of 5 mice per cage. At 6-weeks of age, mice received either a normal chow diet (ND) composed of 22% kcal from fat, 23% kcal from protein and 55% kcal from carbohydrates (Harlan Tekard, Indianapolis, IN, USA) or a high-fat diet (HFD) composed of 60% kcal from fat, 20% kcal from protein and 20% kcal from carbohydrates (Research Diets INC, New Brunswick, NJ, USA) ad libitum. Mice received either a ND or HFD for a short term 8-week or a 22-week long term feeding period (Figure 2a).

Antioxidant treatment with N-acetyl-L-cysteine (NAC) (Santa Cruz Biotechnology, Inc., Santa Cruz, CA, USA) was administered to both ND and HFD groups either in a prevention (pNAC) or intervention (iNAC) treatment. For pNAC treatment, mice received NAC 1 week prior to HFD and treated through 8-week (pNAC-HFD8) or 22-week (pNAC-HFD22) periods (Figure 2b). For iNAC treatment, mice received NAC at week 12 of HFD and continued NAC intake for the duration of the 22-week HFD (iNAC-HFD) (Figure 2b). ND controls were treated in parallel. Initially two NAC dosages at 10 and 50mM were tested (Falach-Malik et al., 2016; Shen et al., 2019). The 50mM dosage was determined to be an effective treatment so this study focused on using 50mM NAC in drinking water for all antioxidant treatment groups. NAC-supplemented drinking water was replaced weekly. NAC intake was assessed in each antioxidant treatment group (over a three-day period) by measuring the difference in volume of water placed in the cage at the beginning of the three-day period compared to the end. This was done two to three weeks after beginning NAC treatment and at the end of each experimental treatment. Data are expressed as NAC intake mg per mouse per day (Shen et al., 2019).

All mice were maintained on a 12-hour light/12-hour dark cycle. Weekly body weights were monitored for all groups, food intake was measured over 16 hours at the end of the assigned diet period in each cage by measuring the change in food weight. Total food intake for the cage was multiplied by kilocalories per gram of food (3.3 kcal/g for ND and 5.21 kcal/g for HFD) and divided by total body weight of mice in the cage to get kcal/g of mouse. Kcal/g of mouse was then multiplied by the body weight of each individual mouse in the cage to get kcal/mouse/16hrs. This was then used to calculate kcal/mouse/24 hours. Food intake is expressed as kcal per mouse per day. All animal work was conducted based on approved protocols from the University of Western Ontario Animal User Subcommittee in accordance with the Canadian Council of Animal Care guidelines (Appendix A).

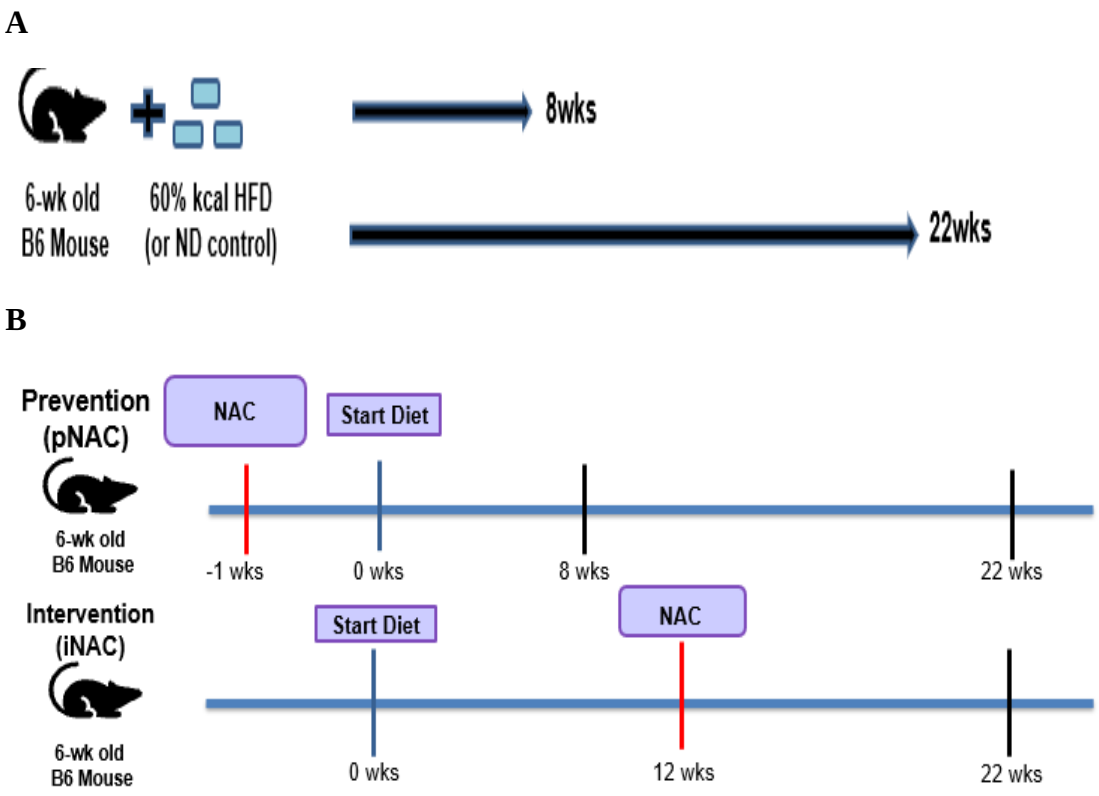

Figure 2.1: Timeline for diet and NAC treatments in intervention and prevention mouse studies.

(A) Male C57Bl/6N mice were fed a 60% kcal HFD for either a short- (8 weeks) or long- (22-weeks) term to assess the progression of glucose and insulin intolerance in mice. Normal diet (ND) controls were treated in parallel. (B) Mice were treated using antioxidant NAC for 1-week before a short term or long term HFD feeding period as prevention treatment (pNAC) or received NAC as an intervention at week 12 of a 22-week HFD (iNAC). ND mice were treated in parallel.

2.2 *In vivo* metabolic experiments

An intraperitoneal glucose tolerance test (IPGTT) was performed in all experimental groups at 8 or 22 weeks on the assigned treatments. IPGTT was conducted following a 16-hour overnight fast with a 2mg/g bodyweight glucose administration (Dextrose, Sigma, Saint Louis, MO, USA). Glucose levels were measured at baseline (0 minutes) before a glucose injection and at 15-, 30-, 60-, and 120-minutes post-glucose injection using a glucometer (Freestyle Lite, Abbott, Alameda, California, USA). Differences between control and experimental groups were compared using area under the curve (AUC) analyses (Zhi Chao Feng et al., 2015).

An intraperitoneal insulin tolerance test (IPITT) was performed after mice were fasted for 4 hours. 1U/kg bodyweight of insulin (Humulin, Eli Lilly, Toronto, ON, Canada) was administered to mice on the 22-week diet groups, while 0.75 U/kg bodyweight of insulin was administered to the 8-week diet groups. Glucose levels were taken at baseline (0 minutes), and at 15-, 30-, 60- and 120-minute following post-insulin administration. Results were normalized to baseline glucose levels (100%) and AUC values were generated to determine changes in insulin sensitivity. (Zhi Chao Feng et al., 2015).

2.3 ELISA measurements of insulin secretion

The ultrasensitive insulin mouse ELISA kit from ALPCO (Salem, NH, USA) with sensitivity at 0.15ng per ml was used to measure insulin levels from fed cardiac blood plasma in all 22-week diet-only, pNAC and iNAC 22-week 50mM NAC treated groups. Plasma samples were assayed undiluted and all values were reported as ng/ml.

2.4 Tissue collection and immunohistological analysis

Mice were sacrificed following 8 or 22 weeks of their assigned diet. Immediately following CO_2 euthanasia, cardiac blood samples, pancreata, and livers were collected. Pancreas weight was also measured at the time of dissection. Pancreas and liver samples were washed with saline before overnight fixation in 4% paraformaldehyde (Fisher Scientific Company, Ottawa, ON, Canada). Tissue samples were processed by a standard protocol of dehydration and paraffin embedding using an automated tissue processing

and embedding machine (Shandon Citadel™ Tissue Processor, Citadel 1000, Thermo Electron Corporation, Waltham, MA, USA). Parrafin blocks were sectioned consecutively at 4-µm with a microtome (Leica RM2245, Vashaw Scientific Inc.; Norcross, Atlanta, USA) throughout the length of the pancreas.

For immunofluorescence (IF) staining, paraffin sections were deparaffinized in xylene, rehydrated with decreasing concentrations of ethanol (from 100% to 70%) and rinsed with running water and 1x phosphate-buffered saline (PBS). Nonspecific binding was blocked using 10% normal goat serum diluted in 1x PBS at room temperature for 30 minutes in a humidified chamber. Sections were incubated with the appropriate dilutions of primary antibodies as listed in **Table 1** overnight at 4^{o}C. As required, 0.2% Triton treatment and/or microwave antigen retrieval with citric acid solution (pH 6.0) were applied to improve detection. Secondary antibodies fluorescein isothiocyanate (FITC) and tetramethyl rhodamine isothiocyanate (TRITC) secondary antibodies (Jackson Immunoresearch, West Grove, PA, USA) were applied for primary detection at 1:50 dilution. 4'-6'-diamidino-2-phenylindole (DAPI) was applied for nuclear counterstaining (1:1000 dilution). Negative controls included the omission of the primary or secondary antibodies; these tests resulted in negative staining reactions, with some background staining when mouse derived FITC was used on mouse tissue (Appendix D).

Images of sections were captured by a Leica DMIRE2 fluorescent microscope (Leica Microsystems, Concord, Ontario, CA). Analysis of islet structure and beta-cell markers was conducted using Image Pro Plus software (Media Cybernetics, Rockville, MD, USA). For αSMA staining, images were obtained using the Nikon Eclipse Ti2 confocal microscope (Nikon, Melville, NY, USA) and quantified using Nikon NIS-Elements software (Nikon, Melville, NY, USA).

Picrosirius Red staining for collagen detection was applied to pancreas and liver samples using the protocol included with the Picro Sirius Red Kit (Connective Tissue Stain) (Abcam, Cambridge, MA, USA).

2.5 Morphometric analysis

Islet morphology was assessed with insulin and glucagon co-staining sections. An islet was defined as three insulin-positive cells and one glucagon-positive cell. All islets in each section were counted and divided by pancreas area to calculate islet density expressed as islet number per square millimeter of pancreatic section (islet#/mm^2). Alpha and beta cell mass was calculated using the following formula: Alpha or Beta cell mass = [Glucagon-positive area or insulin-positive area x pancreas mass (mg)]/ Pancreatic area (mm^2) (Wang et al., 1994). Beta cell size was calculated by dividing the total insulin-positive islet area by the number of insulin-positive cells in ten representative islets per section, while beta cell number was calculated by dividing the number of insulin-positive cells by insulin-positive area in ten representative islets.

Quantification of proliferation (Ki67) and nuclear transcription factors PDX-1 was accomplished through double IF staining with insulin. Double positive cells (Nuclear marker-positive/insulin-positive) were divided by the total insulin-positive cell population in islets and expressed as a percentage (Feng et al., 2012). To quantify the percentage of activated PaSC marker αSMA present in the islets, the positive intra-islet αSMA^+ cell area (μm^2) was manually traced using Nikon NIS-Element software and divided by the total insulin-positive area (μm^2) (Lee et al., 2017).

2.6 Statistical Analysis

ND and HFD groups were compared initially using an unpaired student's t-test to establish the model. All diet groups with or without NAC treated were compared using one-way ANOVA in GraphPad Prism 5.0 followed by Tukey's Post-Hoc test (GraphPad Software, Inc., La Jolla, CA, USA). All data is expressed as means ± SEM and statistical significance was obtained when $p<0.05$.

Table 2.1. List of Antibodies Used for Immunofluorescence (IF) Staining Analyses

Primary Antibody	Catalogue Number	Dilution	Company
Mouse Anti-αSMA†	Ab7817	1:100	Abcam (Cambridge, MA, USA)
Rabbit Anti-Glucagon	Sab4501137	1:100	Sigma-Aldrich (St Louis, MO, USA)
Rabbit Anti-Insulin	Sc-9168	1:50	Santa Cruz (Santa Cruz, CA, USA)
Mouse Anti-Insulin	I2018	1:800	Sigma-Aldrich (St Louis, MO, USA)
Rabbit Anti-Insulin	C27c9	1:400	Cell Signaling (Temecula, CA, USA)
Rabbit Anti-Ki67*	Ab15580-100	1:100	Abcam (Cambridge, MA, USA)
Rabbit Anti-Pdx-1*	Gift	1:800	Dr. Christopher V. Wright (University of Vanderbilt, Nashville, TN, USA)
		Secondary Antibodies	
FITC Goat anti-mouse	115095062	1:50	JRL (West Grove, PA, USA)
FITC Goat anti-rabbit	111095045	1:50	JRL (West Grove, PA, USA)
TRITC Goat anti-mouse	115025062	1:50	JRL (West Grove, PA, USA)
TRITC Goat anti-rabbit	111025045	1:50	JRL (West Grove, PA, USA)

* Indicates microwave antigen retrieval was required; ł indicates 0.2% triton treatment

Chapter 3

3 Results

3.1 HFD induced a progressive metabolic dysfunction mouse model of T2DM

In order to establish when glucose and insulin intolerance appeared during diet-induced T2DM progression in 6-week old male B6 mice fed a 60% kcal HFD for an 8-week or 22-week period. After an 8-week dietary treatment, HFD mice exhibited significantly increased body weight (Figure 3.1a) and higher fasted blood glucose levels (Figure 3.1b) compared to the ND group. Significantly impaired glucose tolerance (Figure 3.1c), but not insulin tolerance (Figure 3.1d), was observed in 8-week HFD mice, suggesting that insulin resistance has not yet developed in HFD mice during this period.

After 22 weeks of diet treatment, HFD mice showed an increase in both final body weight (Figure 3.2a) and fasted blood glucose levels (Figure 3.2b) compared to ND controls. These mice also demonstrated increased non-fasted plasma insulin levels (Figure 3.2c). Both impaired glucose and insulin tolerance were observed in HFD mice when compared to ND mice (Figure 3.2d and 3.2e). Taken together, this data indicates that long-term HFD feeding induces glucose intolerance and insulin resistance in mice similar to the pre-diabetic phenotype observed in human T2DM patients.

Figure 3.1 Effect of ND and HFD on body weight and glucose metabolism following 8 weeks of diet treatment

(a) Weekly body weights of mice on ND or HFD for 8 weeks were taken and compared during dietary treatment (*n=7-10* mice per experimental group). (b) Blood glucose levels were measured following a 16-hour overnight fast after 8 weeks of diet treatment (*n=10-14* mice per experimental group). (c) Glucose and (d) insulin tolerance tests were assessed using an intraperitoneal glucose (IPGTT) or insulin (IPITT) injection followed by statistical analysis of the area under the curve (AUC) (*n=7-10* mice per experimental group). Data were compared using unpaired Student's t-tests and determined to be significant at *$p<0.05$, **$p<0.01$ vs. ND mice. All data are expressed as means ±SEM. Black solid circle, ND mice; black solid square, HFD mice.

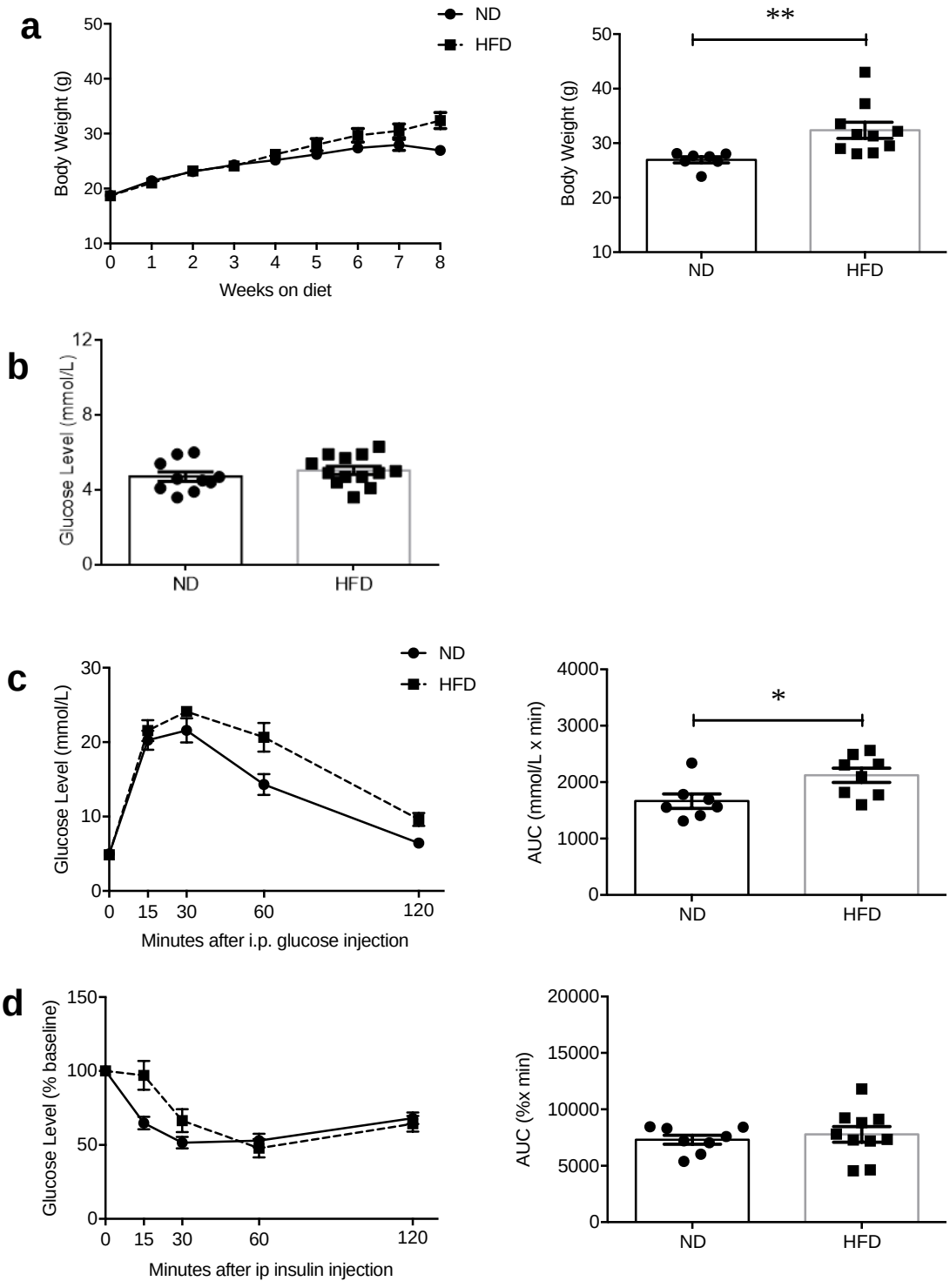
a
ND
HFD
Body Weight (g)
Weeks on diet
**
Body Weight (g)
ND
HFD
b
Glucose Level (mmol/L)
ND
HFD
c
ND
HFD
Glucose Level (mmol/L)
Minutes after i.p. glucose injection
*
AUC (mmol/L x min)
ND
HFD
d
Glucose Level (% baseline)
Minutes after ip insulin injection
AUC (%x min)
ND
HFD

Figure 3.1

Figure 3.2 Effect of ND and HFD on body weight and glucose metabolism following 22 weeks of diet treatment

(a) Biweekly body weights of mice on ND or HFD treatment for 22 weeks (left) and final body weight of mice at 22 weeks (right) were compared (*n=10-17* mice per experimental group). (b) Blood glucose levels at 22 weeks of diet were measured following a 16-hour overnight fast. (*n=8-10* mice per experimental group). (c) Non-fasted plasma insulin levels were examined at the end of 22 weeks. (*n=5-6* mice per experimental group). (d) Glucose and (e) insulin tolerance were assessed using an intraperitoneal glucose or insulin injection followed by statistical analysis of the area under the curve (AUC). (*n=6-10* mice per experimental group). All data are expressed as means ±SEM and compared using unpaired Student's t-tests. *$p<0.05$, **$p<0.01$, ***$p<0.001$ vs. ND mice. Black solid circle, ND mice; black solid square, HFD mice.

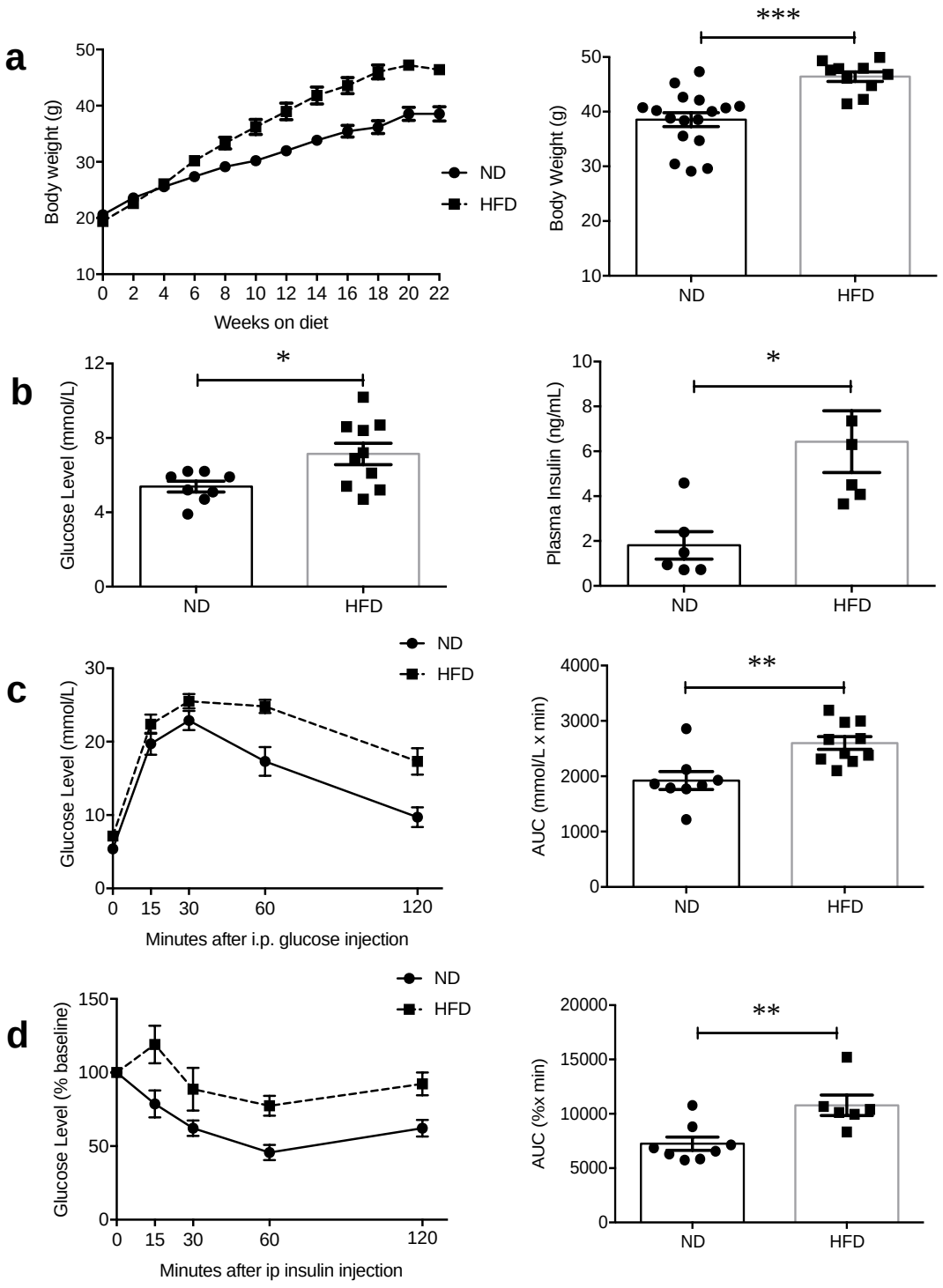
a
Body weight (g)
Weeks on diet
ND
HFD
***
Body Weight (g)
b
Glucose Level (mmol/L)
*
Plasma Insulin (ng/mL)
c
Glucose Level (mmol/L)
Minutes after i.p. glucose injection
**
AUC (mmol/L x min)
d
Glucose Level (% baseline)
Minutes after ip insulin injection
AUC (%x min)

Figure 3.2

3.2 NAC administration did not change caloric intake during prevention and intervention treatments

NAC intake in mice fed ND or HFD was not significantly altered in either the 8-week or 22-week diet groups (Figure 3.3). The average NAC intake was similar between ND and HFD groups (18-18.7 mg/mouse/day) during prevention treatment (Figure 3.3a). Intervention NAC treatment in ND-fed mice was slightly higher (16 mg/mouse/day) compared to HFD mice (14 mg/mouse/day) but did not reach statistical significance (Figure 3.3b). The caloric intake in prevention and intervention groups with diet controls for 8 or 22 weeks was monitored. No significant change in caloric intake between ND and ND+pNAC mice and between HFD and HFD+pNAC mice on 8 weeks prevention treatment was detected, but HFD+pNAC mice had high caloric intake when compared to ND and ND+pNAC groups (Figure 3.4a). Long term NAC prevention did not alter caloric intake in both ND+pNAC and HFD+pNAC mice after 22 weeks of prevention treatment when compared to untreated groups (Figure 3.4b), suggesting that NAC treatment at long-term administration does not influence caloric intake in either ND and HFD mice. Caloric intake in intervention NAC treatment groups showed no change between ND and ND+iNAC or between HFD and HFD+iNAC groups, however, HFD+iNAC displayed high level caloric intake compared to both ND groups (Figure 3.4c).

Figure 3.3 NAC intake was similar between diet- and NAC-treated groups in both prevention and intervention studies.

Average NAC intake for mice undergoing (a) prevention and (b) intervention treatment. All data were compared using unpaired Student's t-tests and expressed as means ±SEM. (*n=4-9* mice per experimental group). Blue open circle, ND plus NAC mice; red open square, HFD plus NAC mice. pNAC, prevention study; iNAC, intervention study.

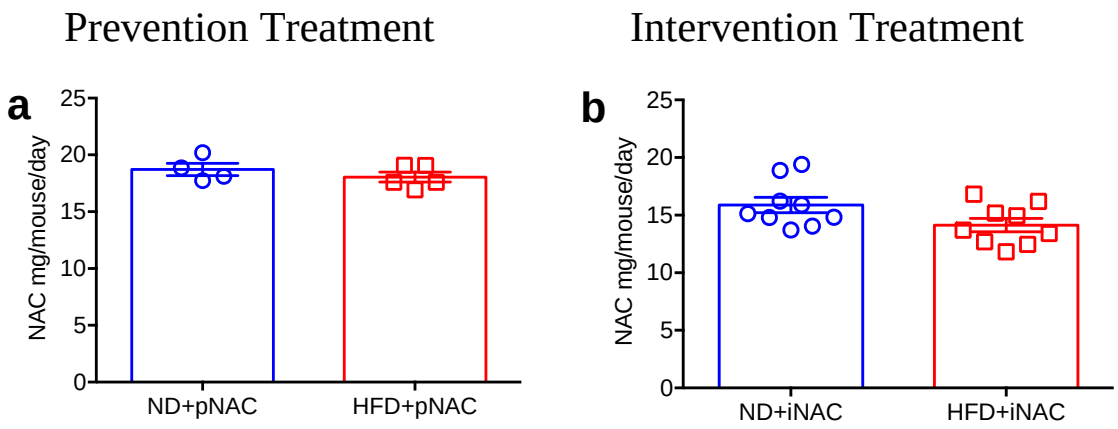
Prevention Treatment
Intervention Treatment
a
b
NAC mg/mouse/day
25
20
15
10
5
0
ND+pNAC
HFD+pNAC
ND+iNAC
HFD+iNAC

Figure 3.3

Figure 3.4 Caloric intake in diet- and NAC-treated groups in both prevention and intervention studies.

Average caloric (kcal) intake for mice undergoing a (a) short-term (8 weeks) or (b) long-term (22 weeks) prevention study in ND and HFD mice. (c) Average caloric intake for ND and HFD mice on intervention NAC treatment at 22 weeks. All data were compared using a one-way ANOVA with Tukey Post-Hoc and expressed as means ±SEM. Significance was determined at *$p<0.05$, **$p<0.01$. (*n=3-13* mice per experimental group). Black solid circle, ND mice; black solid square, HFD mice; blue open circle, ND plus NAC mice; red open square, HFD plus NAC mice. pNAC, prevention study; iNAC, intervention study.

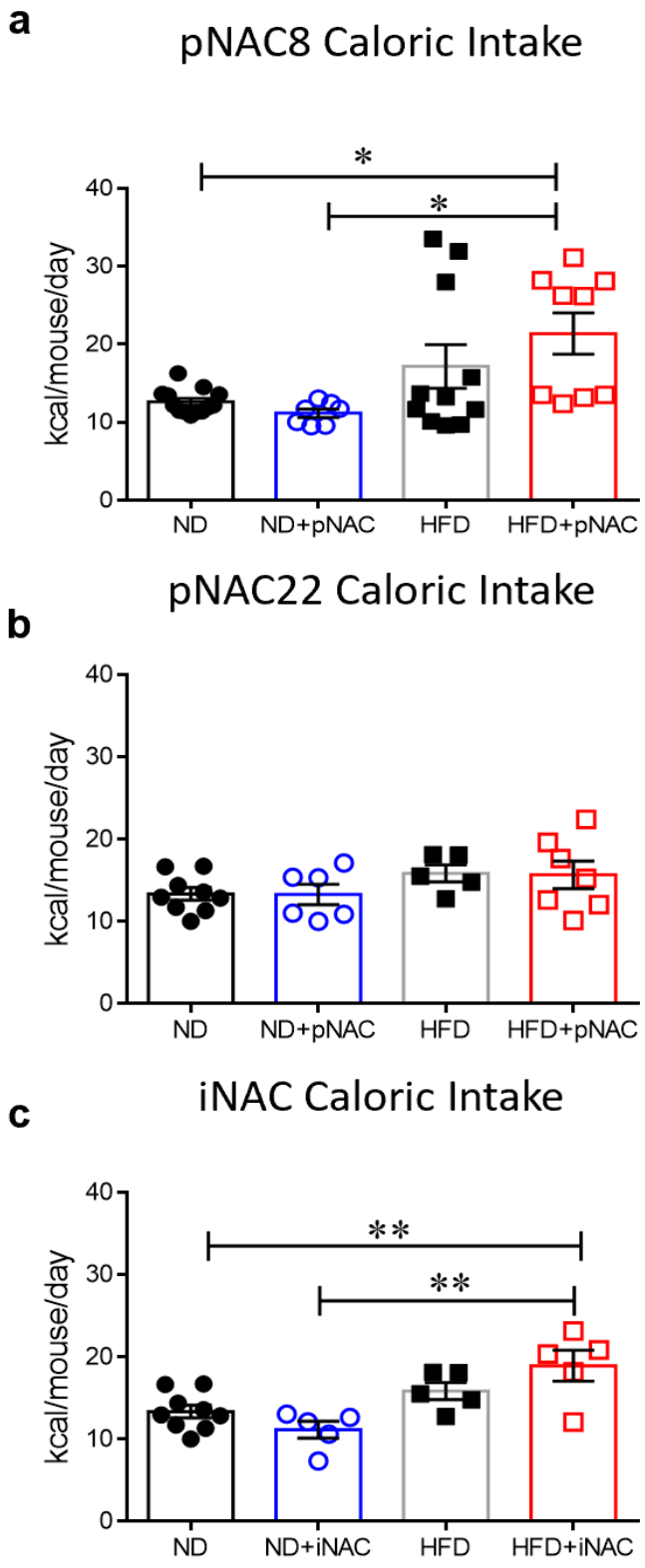
a
pNAC8 Caloric Intake
kcal/mouse/day
0
10
20
30
40
*
*
ND
ND+pNAC
HFD
HFD+pNAC
b
pNAC22 Caloric Intake
kcal/mouse/day
0
10
20
30
40
ND
ND+pNAC
HFD
HFD+pNAC
c
iNAC Caloric Intake
kcal/mouse/day
0
10
20
30
40
**
**
ND
ND+iNAC
HFD
HFD+iNAC

Figure 3.4

3.3 Preventative NAC treatment for 8-week HFD did not affect glucose or insulin tolerance

Antioxidant NAC treatment was administered one week prior to the start of an 8-week HFD in order to determine whether a reduction in oxidative stress could improve glucose tolerance. Body weight was monitored weekly (Figure 3.5a). In ND+pNAC mice body weight was reduced compared to ND, but no significant change in body weight was observed between HFD and HFD+pNAC mice (Figure 3.5b). Fasted blood glucose levels were unchanged when comparing between ND and ND+pNAC or HFD and HFD+pNAC groups (Figure 3.5c). Glucose tolerance tests demonstrated similar response between ND and ND+pNAC mice as well as between HFD and HFD+pNAC mice. However, HFD-pNAC glucose tolerance was significantly worsened compared to ND+pNAC (Figure 3.6a and 6b). Insulin tolerance was not significantly altered, although an improvement at 30 minutes following intra-peritoneal insulin injection was found in HFD+pNAC mice when compared to HFD mice (Figure 3.6c and 6d).

Figure 3.5 Body weight and fasted blood glucose levels following NAC prevention treatment in ND or HFD for 8 weeks.

(a) Weekly body weights were taken for ND, ND+pNAC, HFD, and HFD+pNAC mice during 8-week prevention treatment. (*n=4-9* mice per experimental group). (b) Body weight and (c) fasted blood glucose levels for 8-week ND, ND+pNAC, HFD, and HFD+pNAC mice (*n=3-9* mice per experimental group). ND and HFD are the same values from figure 3.1. All data were compared using one-way ANOVA with Tukey Post-Hoc and expressed as means ±SEM and determined to be significant at *$p<0.05$, **$p<0.01$. Black solid circle, ND mice; black solid square, HFD mice; blue open circle, ND+pNAC mice; red open square, HFD+pNAC mice. pNAC, prevention study.

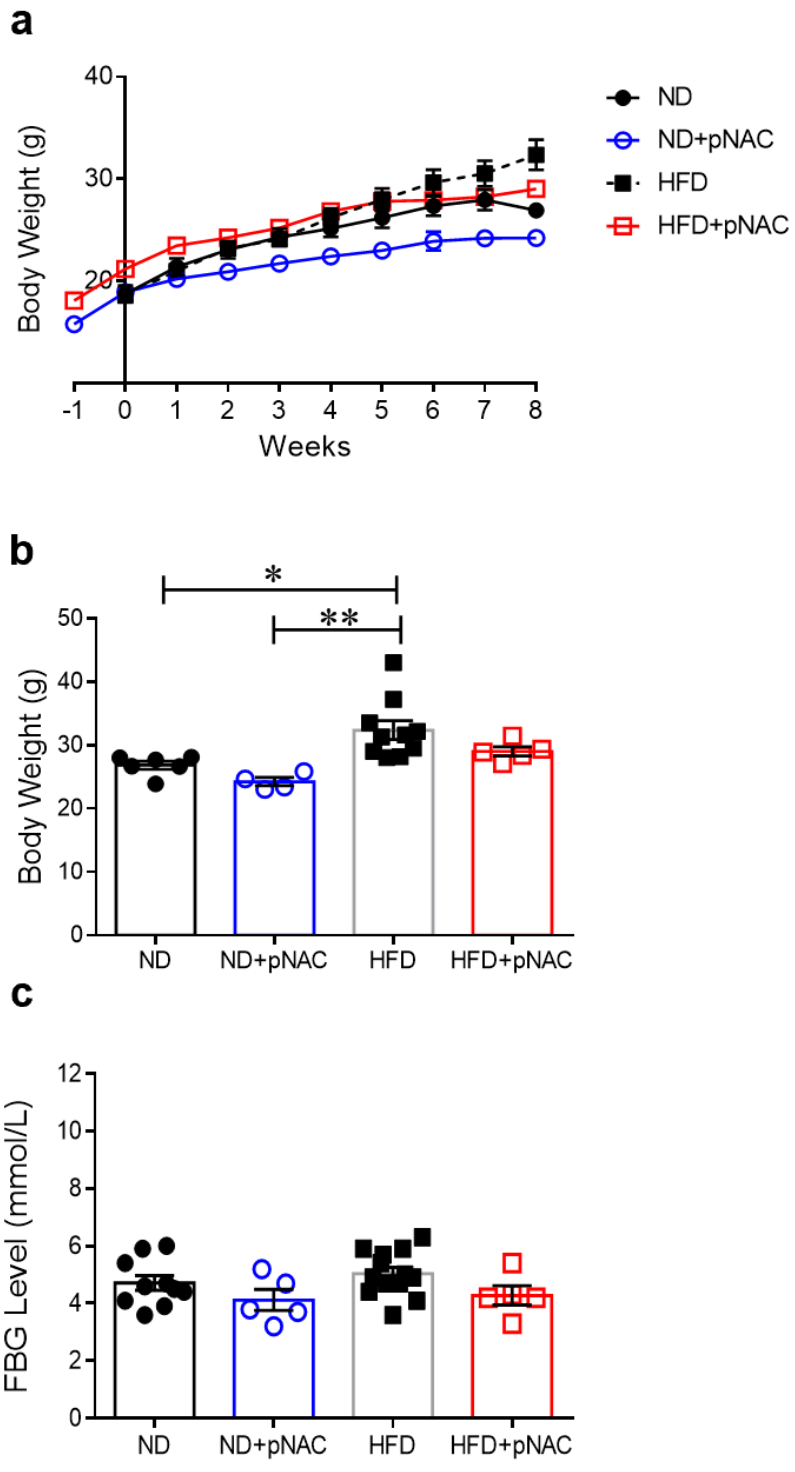
a
Body Weight (g)
40
30
20
-1
0
1
2
3
4
5
6
7
8
Weeks
ND
ND+pNAC
HFD
HFD+pNAC
b
Body Weight (g)
*
**
50
40
30
20
10
0
ND
ND+pNAC
HFD
HFD+pNAC
c
FBG Level (mmol/L)
12
10
8
6
4
2
0
ND
ND+pNAC
HFD
HFD+pNAC

Figure 3.5

Figure 3.6 NAC prevention treatment for 8 weeks did not restore glucose tolerance in HFD–fed mice.

(a) IPGTT results from ND, ND+pNAC, HFD, and HFD+pNAC mice during 8-week experiment and (b) area under curve (AUC) analysis of IPGTT. (*n=3-8* mice per experimental group). (c) IPITT results from ND, ND+pNAC, HFD, and HFD+pNAC mice during 8-week prevention and (d) AUC analysis of IPITT. (*n=4-8* mice per experimental group). ND and HFD are the same values from figure 3.1. All data were compared using a one-way ANOVA with Tukey Post-Hoc and expressed as means ±SEM. Significance was determined at *$p<0.05$, **$p<0.01$. Black solid circle, ND mice; black solid square, HFD mice; blue open circle, ND+pNAC mice; red open square, HFD+pNAC mice. pNAC, prevention study.

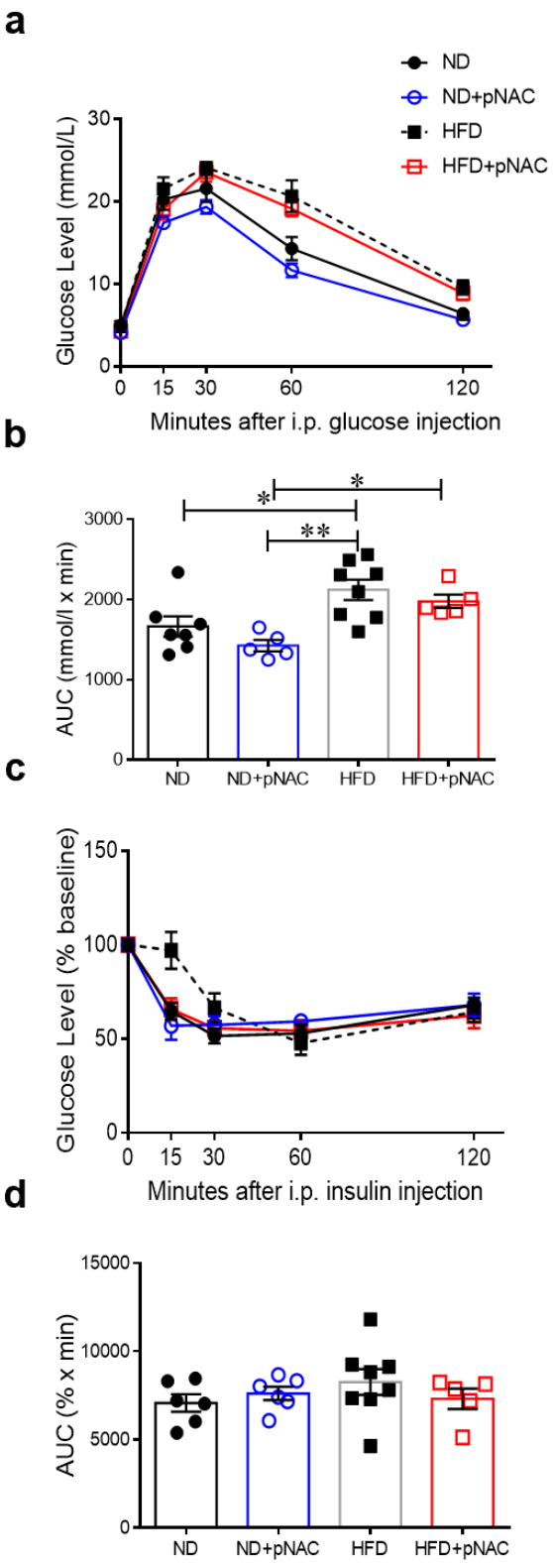
a
ND
ND+pNAC
HFD
HFD+pNAC
Glucose Level (mmol/L)
30
20
10
0
0 15 30 60 120
Minutes after i.p. glucose injection
b
*
*
**
AUC (mmol/l x min)
3000
2000
1000
0
ND ND+pNAC HFD HFD+pNAC
c
Glucose Level (% baseline)
150
100
50
0
0 15 30 60 120
Minutes after i.p. insulin injection
d
AUC (% x min)
15000
10000
5000
0
ND ND+pNAC HFD HFD+pNAC

Figure 3.6

3.4 Preventative NAC treatment affected islet morphology, beta cell proliferation, and islet PaSCs under ND and HFD for 8 weeks

Morphological analysis of islet density in the pancreas of ND, HFD and HFD+pNAC mice was similar, yet ND+pNAC mice showed a reduction in islet density when compared to ND islets (Figure 3.7a). There was no significant alteration of islet architecture between the experimental groups, as determined by the double immunofluorescence staining of insulin and glucagon (Figure 3.7b). Although HFD mice showed lower beta and alpha cell mass than that of ND group, similar alpha and beta cell mass was detected between HFD and HFD+pNAC mice (Figure 3.7c and 7d). Interestingly reduced beta and alpha cell mass was observed in ND+pNAC mice when compared to ND mice, although this did not reach statistical significance (Figure 3.7c and 7d). Low sample sizes should be considered when interpreting the changes seen at this time point. Co-staining of Ki67, a marker of proliferation with insulin positive cells showed no change in ND+pNAC compared to ND following 8 weeks of diet, but a reduction of beta cell proliferation in HFD+pNAC compared to HFD samples (Figure 3.8a and 8b). Additionally, mice fed a HFD exhibited an increased intra-islet αSMA^{+} area compared to ND, which was significantly decreased using HFD+pNAC (Figure 3.9).

Figure 3.7 Islet density was significantly decreased in 8-week ND mice on a NAC prevention treatment.

(a) The number of islets in the pancreas of experimental groups on 8-week pNAC treatment. (*n=3* mice per experimental group). (b) Representative double immunofluorescence images for glucagon (green) and insulin (red) staining for ND, ND+pNAC, HFD and HFD+pNAC treated pancreata. DAPI (blue) was used to label nuclei. Scale bar, 50 μm. Morphometric quantification of (c) beta and (d) alpha cell mass of all experimental groups. (*n=3-5* mice per experimental group). All data are compared using one-way ANOVA with Tukey Post-Hoc and expressed as means ±SEM. Black solid circle, ND mice; black solid square, HFD mice; blue open circle, ND+pNAC mice; red open square, HFD+pNAC mice. pNAC, prevention study.

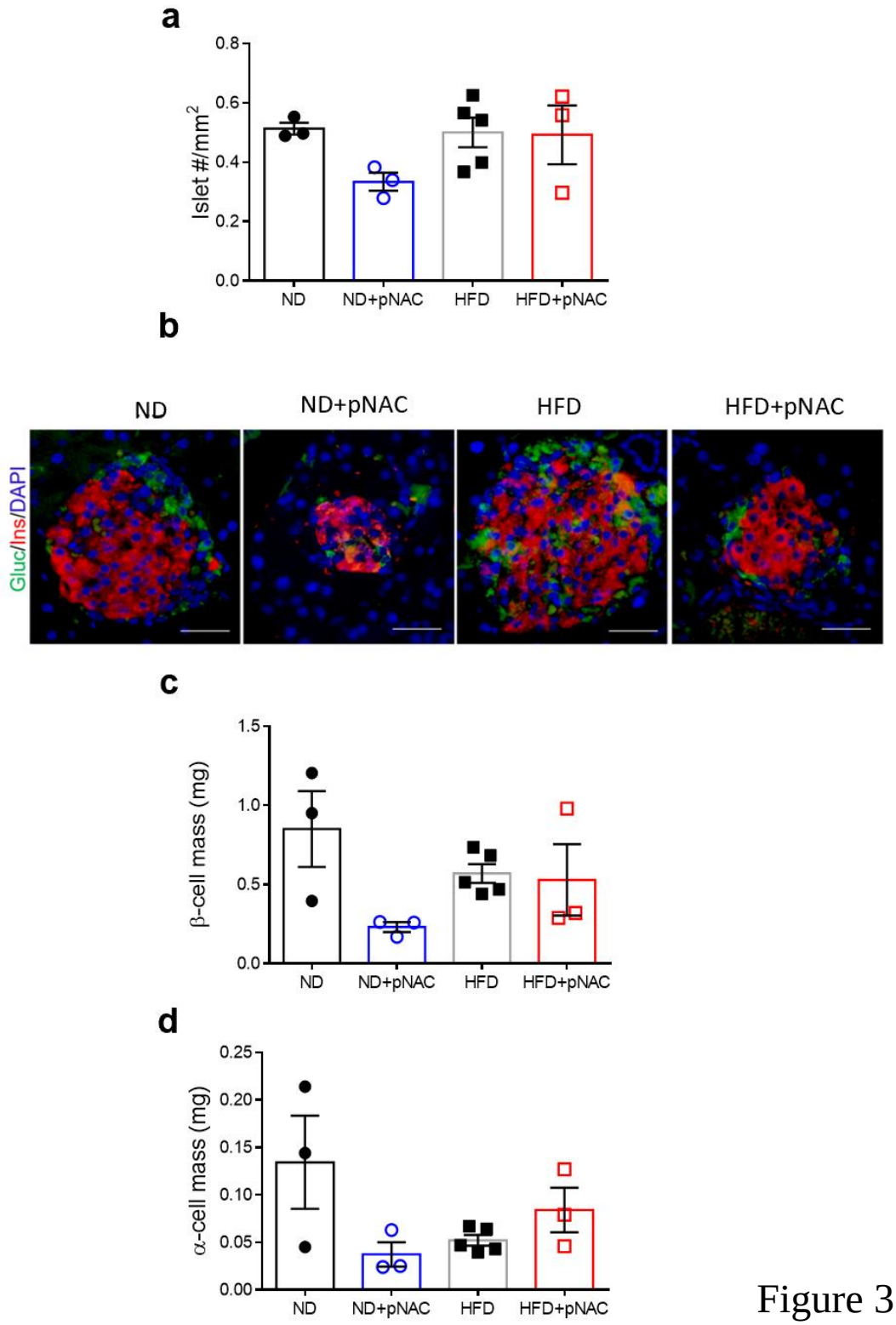
a
Islet #/mm2
0.8
0.6
0.4
0.2
0.0
ND
ND+pNAC
HFD
HFD+pNAC
b
ND
ND+pNAC
HFD
HFD+pNAC
Gluc/Ins/DAPI
c
β-cell mass (mg)
1.5
1.0
0.5
0.0
ND
ND+pNAC
HFD
HFD+pNAC
d
α-cell mass (mg)
0.25
0.20
0.15
0.10
0.05
0.00
ND
ND+pNAC
HFD
HFD+pNAC

Figure 3.7

Figure 3.8 Beta-cell proliferation in 8-week ND and HFD mice on a NAC prevention treatment.

(a) Representative double immunofluorescence images for Ki67 (green) and insulin (red) staining for ND, ND+pNAC, HFD and HFD+pNAC treated pancreata. DAPI, blue. Scale bar, 50 μm. Asterisks represent non-specific blood staining and arrows indicate positive signaling. (b) Percentage of Ki67 and insulin positive co-stained cells over total insulin positive cells for beta cell proliferation in the islets of ND mice compared to ND+pNAC mice and HFD mice compared to HFD+pNAC mice. All data are compared using one-way ANOVA with Tukey Post-Hoc and expressed as means ±SEM (*n= 3* mice per experimental group). Black solid circle, ND mice; black solid square, HFD mice; blue open circle, ND+pNAC mice; red open square, HFD+pNAC mice. pNAC, prevention study.

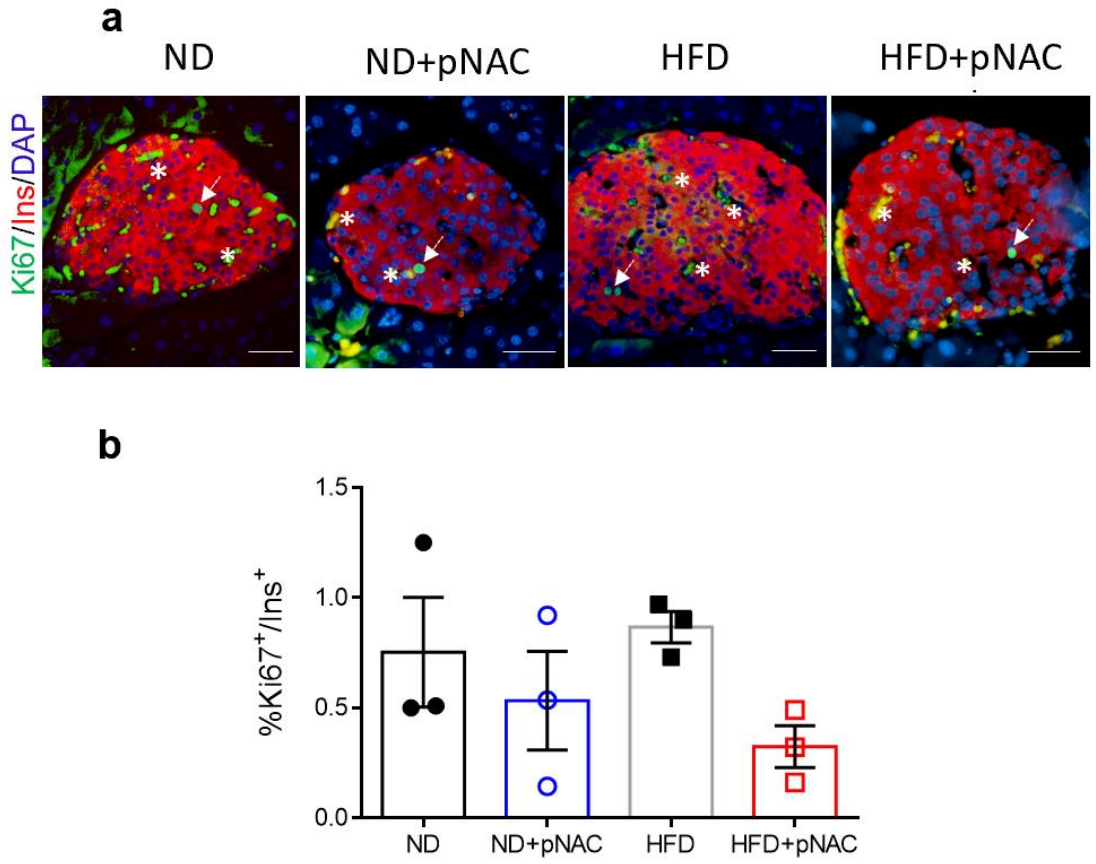
a
ND
ND+pNAC
HFD
HFD+pNAC
Ki67/Ins/DAP
b
%Ki67+/Ins+
1.5
1.0
0.5
0.0
ND
ND+pNAC
HFD
HFD+pNAC

Figure 3.8

Figure 3.9 PaSC activation was reduced in HFD mouse islets following preventive NAC treatment for 8 weeks.

(a) Quantitative analysis of activated PaSCs, labeled by αSMA, in the islets of ND, ND+pNAC, HFD and HFD+pNAC groups. Representative double immunofluorescence images for (b) αSMA (green) with insulin (red) with αSMA (green) only images below. DAPI stained in blue. Scale bar, 50 μm. All data are compared using one-way ANOVA with Tukey Post-Hoc and determined to be significant at *$p<0.05$. Data expressed as means ±SEM (*n= 3* mice per experimental group). Black solid circle, ND mice; black solid square, HFD mice; blue open circle, ND+pNAC mice; red open square, HFD+pNAC mice. pNAC, prevention study.

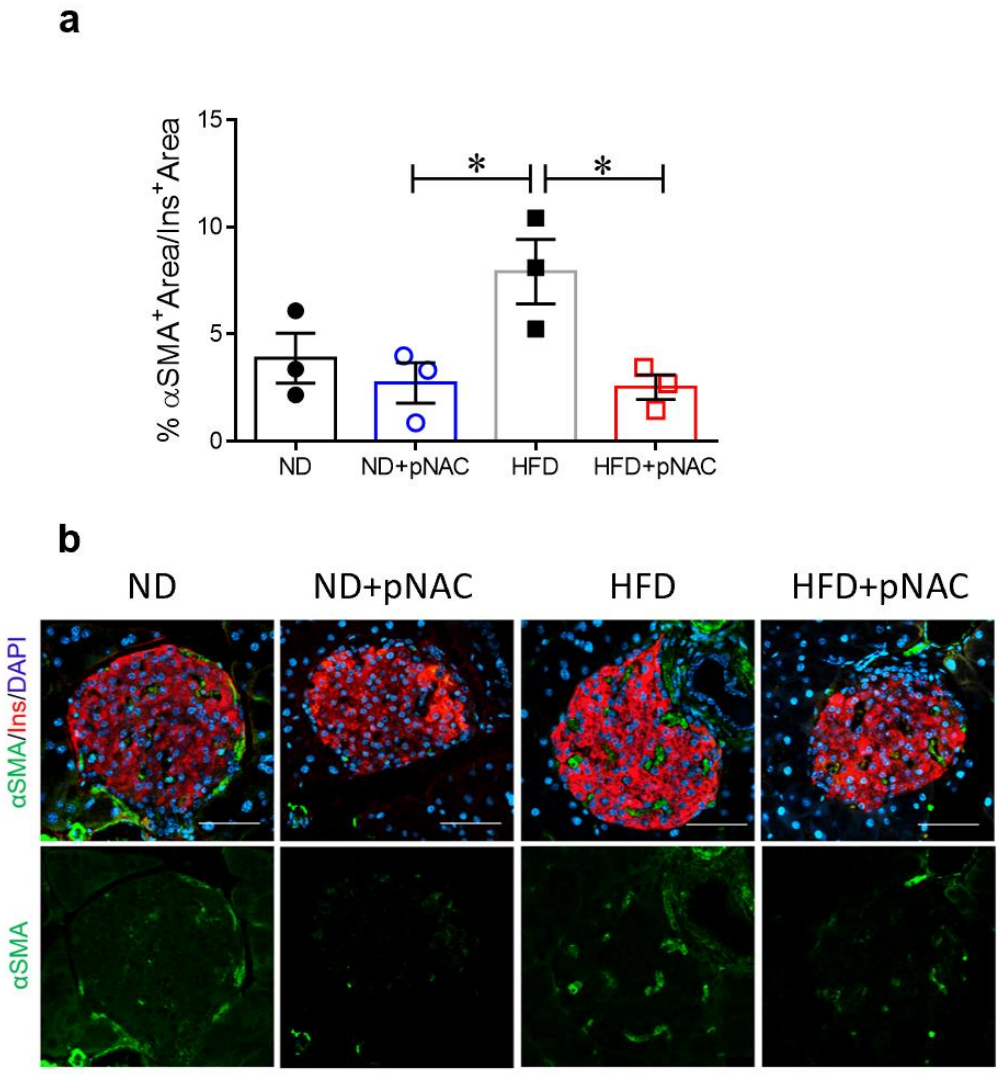
a
% αSMA+Area/Ins+Area
15
10
5
0
*
*
ND
ND+pNAC
HFD
HFD+pNAC
b
ND
ND+pNAC
HFD
HFD+pNAC
αSMA/Ins/DAPI
αSMA

Figure 3.9

3.5 Preventative NAC treatment for a 22-week HFD improved mouse glucose and insulin tolerance

Due to the early nature of the 8-week time point, which did not demonstrate an improvement with short-term NAC treatment, the NAC prevention study was extended throughout 22 weeks of HFD feeding to determine whether significant improvements could be found with a longer treatment and when compared to a progressively glucose intolerant phenotype. Bi-weekly body weight was monitored for 22 weeks of diet and showed that NAC treatment reduced body weight in both ND+pNAC and HFD+pNAC compared to ND and HFD mice, respectively (Figure 3.10a and b). ND+pNAC mice showed no significant changes in fasting blood glucose, glucose tolerance, or insulin resistance when compared to ND mice (Figure 3.10 and 3.11). Preventive NAC treatment in HFD mice (HFD+pNAC) displayed lower fasted blood glucose level and circulating plasma insulin levels compared to HFD mice (Figure 3.10c,d). Furthermore, HFD+pNAC treatment was able to significantly improve glucose tolerance and insulin tolerance when compared to HFD mice (Figure 3.11). At the islet level, improvements in beta cell mass (Figure 3.12b,c) and intra-islet αSMA positive area were observed (Figure 3.12).

Figure 3.10 Effect of preventative NAC treatment on body weight and fasted blood glucose level following 22 weeks of diet.

(a) Bi-weekly body weights were measured in ND, ND+pNAC, HFD and HFD+pNAC mice during 22-week treatment. (b) Body weight and (c) fasted blood glucose levels at 22-week in ND, ND+pNAC, HFD, and HFD+pNAC treated mice. (*n=3-17* mice per experimental group). (d) Non-fasted plasma insulin levels were examined at the end of the experiments (*n=3-6* mice per experimental group). ND and HFD are the same values from figure 3.2. All data were compared using a one-way ANOVA with Tukey Post-Hoc and expressed as means ±SEM. Significance was determined at *$p<0.05$, **$p<0.01$. Black solid circle, ND mice; black solid square, HFD mice; blue open circle, ND+pNAC mice; red open square, HFD+pNAC mice. pNAC, prevention study.

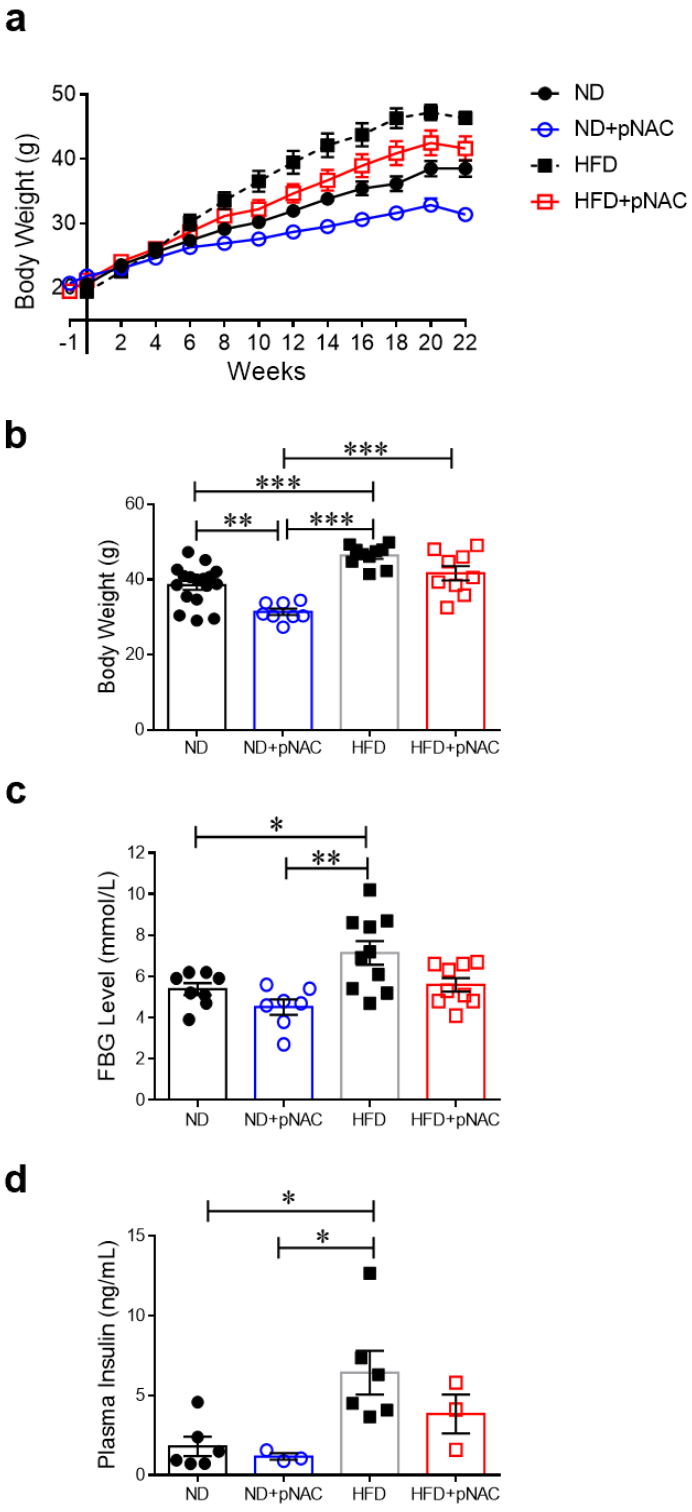
a
Body Weight (g)
Weeks
ND
ND+pNAC
HFD
HFD+pNAC
b
Body Weight (g)
c
FBG Level (mmol/L)
d
Plasma Insulin (ng/mL)

Figure 3.10

Figure 3.11 NAC prevention treatment for 22 weeks restored glucose tolerance in HFD–fed mice.

(a) IPGTT from ND, ND+pNAC, HFD, and HFD+pNAC mice after 22 weeks of treatment and (b) area under curve (AUC) analysis of IPGTT. (*n=7-10* mice per experimental group). (c) IPITT from ND, ND+pNAC, HFD, and HFD+pNAC after 22-week treatment and (d) AUC analysis of IPITT. (*n=6-9* mice per experimental group). ND and HFD are the same values from figure 3.2. All data were compared using a one-way ANOVA with Tukey Post-Hoc and expressed as means ±SEM. Significance was determined at *$p<0.05$, **$p<0.01$. Black solid circle, ND mice; black solid square, HFD mice; blue open circle, ND+pNAC mice; red open square, HFD+pNAC mice. pNAC, prevention study.

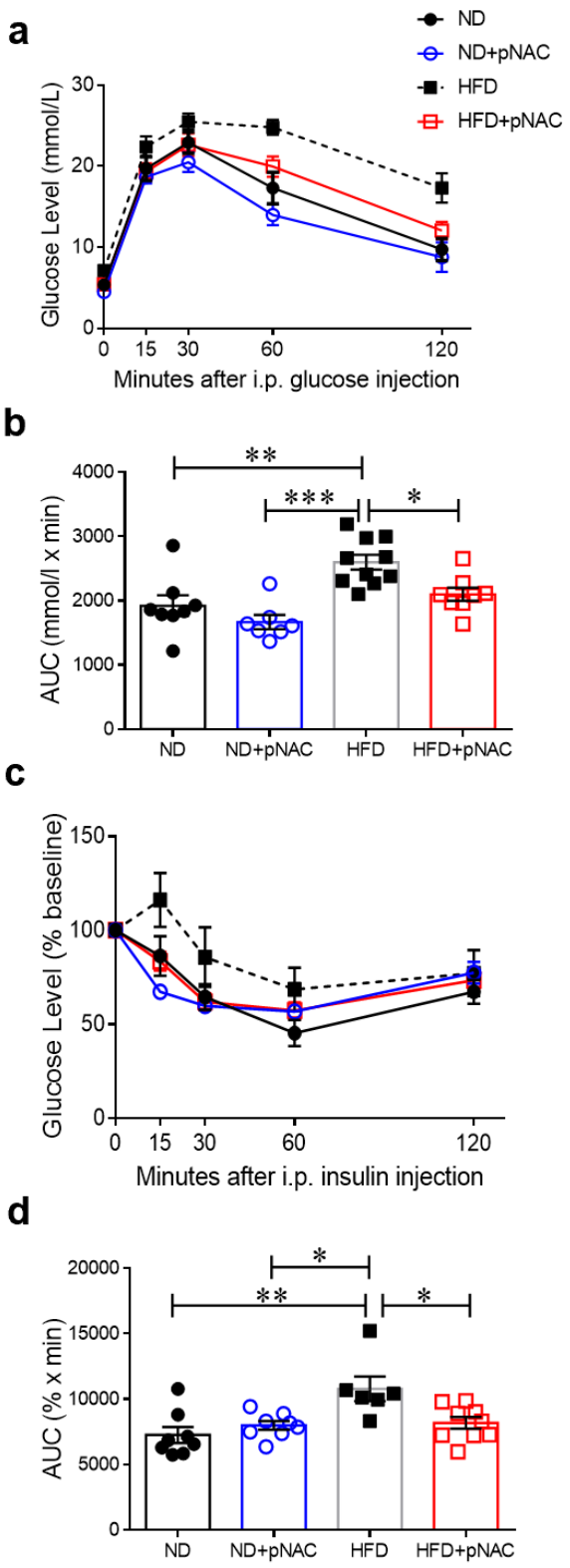
a
ND
ND+pNAC
HFD
HFD+pNAC
Glucose Level (mmol/L)
30
20
10
0
0 15 30 60 120
Minutes after i.p. glucose injection
b
**
***
*
AUC (mmol/l x min)
4000
3000
2000
1000
0
ND
ND+pNAC
HFD
HFD+pNAC
c
Glucose Level (% baseline)
150
100
50
0
0 15 30 60 120
Minutes after i.p. insulin injection
d
*
**
*
AUC (% x min)
20000
15000
10000
5000
0
ND
ND+pNAC
HFD
HFD+pNAC

Figure 3.11

Figure 3.12 Long term NAC prevention treatment for 22 weeks normalizes beta cell mass and reduces intra-islet αSMA staining.

(a) Islet density in the pancreas of experimental groups at 22-week pNAC treatment. (*n=3-5* mice per experimental group). (b) Representative double immunofluorescence images for glucagon (green) and insulin (red) staining for ND, ND+pNAC, HFD and HFD+pNAC treated pancreata. DAPI (blue) was used to label nuclei. Scale bar, 50 μm. (c) Morphometric quantification of beta cell mass of all experimental groups. (*n=3-6* mice per experimental group). (d) Representative double immunofluorescence images for αSMA (green) and insulin (red) for ND, ND+pNAC, HFD and HFD+pNAC treated pancreata. DAPI (blue) was used to label nuclei. Scale bar, 50 μm. All data were compared using a one-way ANOVA with Tukey Post-Hoc and expressed as means ±SEM. Significance was determined at *$p<0.05$, **$p<0.01$. Black solid circle, ND mice; black solid square, HFD mice; blue open circle, ND+pNAC mice; red open square, HFD+pNAC mice. pNAC, prevention study.

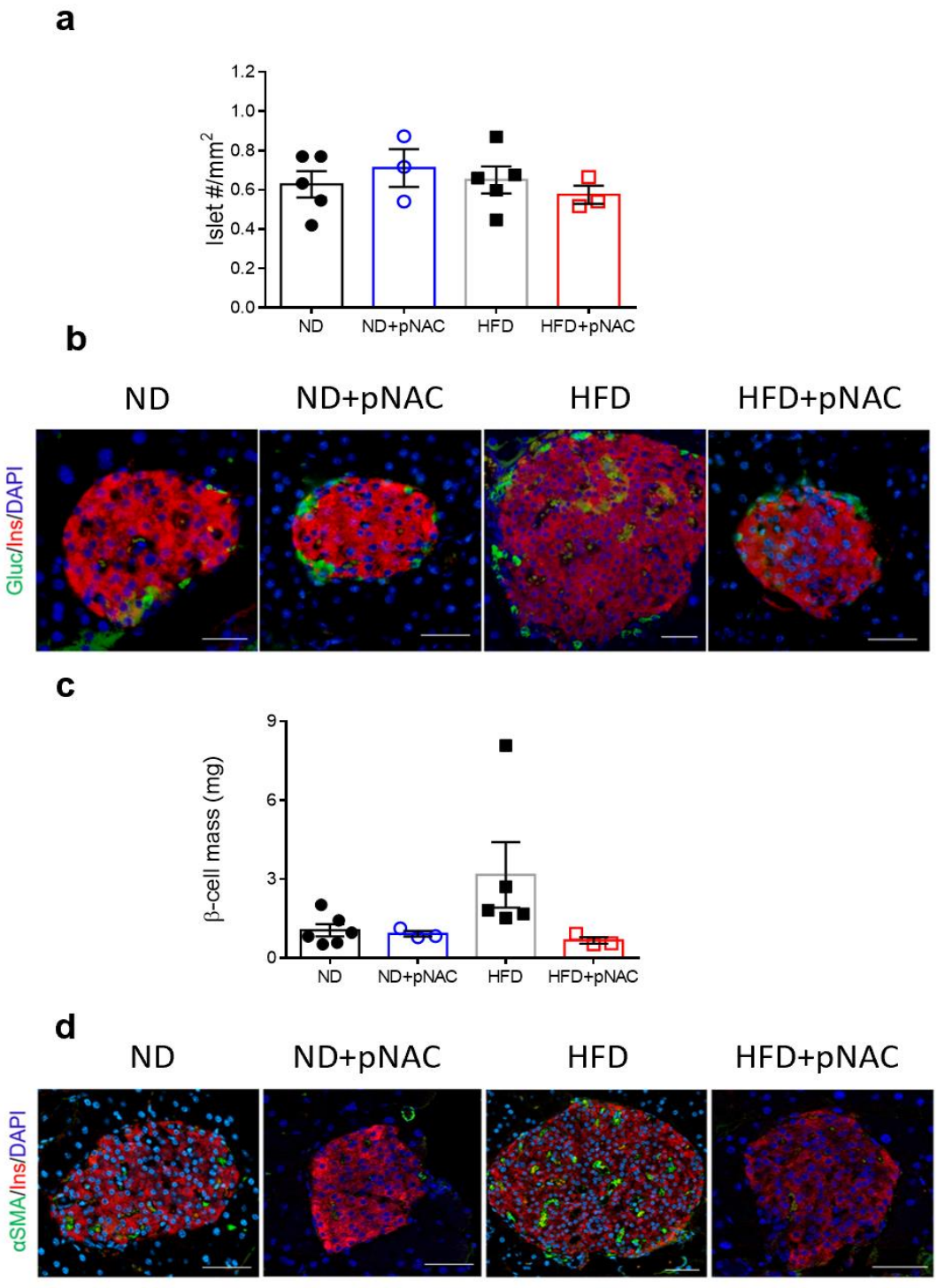
a
Islet #/mm2
1.2
1.0
0.8
0.6
0.4
0.2
0.0
ND
ND+pNAC
HFD
HFD+pNAC
b
ND
ND+pNAC
HFD
HFD+pNAC
Gluc/Ins/DAPI
c
β-cell mass (mg)
9
6
3
0
ND
ND+pNAC
HFD
HFD+pNAC
d
ND
ND+pNAC
HFD
HFD+pNAC
αSMA/Ins/DAPI

Figure 3.12

3.6 Intervention NAC treatment did not improve HFD-induced glucose intolerance

Mice under HFD for 22 weeks demonstrated a progressive T2DM-like phenotype when compared to 8-week HFD mice. After 12 weeks of ND and HFD, mice received NAC as an intervention treatment (iNAC) until 22 weeks following diet. In ND+iNAC mice, a significant reduction in body weight was associated with lower fasting blood glucose when compared to ND mice, but no change to non-fasted plasma insulin levels was detected between the two groups (Figure 3.13). Similar glucose and insulin tolerance were found between ND and ND+iNAC mice (Figure 3.14). There was no difference of body weight and fasted blood glucose level observed between HFD and HFD+iNAC mice, but non-fasted plasma insulin level in HFD+iNAC mice was significantly lower than that of HFD mice (Figure 3.13). It was also noted that there were no improvements in glucose tolerance in the HFD+iNAC group compared to HFD, and HFD+iNAC maintained significantly worsened glucose tolerance compared to ND. While insulin tolerance was not significantly improved in HFD+iNAC compared to HFD, significant change between HFD+iNAC and ND groups was lost (Figure 3.14).

Figure 3.13 Effect of NAC intervention treatment on body weight, blood glucose, and plasma insulin levels following 22 weeks of diet.

(a) Biweekly body weights were measured from ND, ND+iNAC, HFD and HFD+iNAC mice during the 22 weeks of treatment. (*n=7-17* mice per experimental group). (b) Body weight, (c) fasted blood glucose levels, and (d) non-fasted plasma insulin levels were measured at 22 weeks of diet in ND, ND+iNAC, HFD, and HFD+iNAC mice. (*n=6-10* mice per experimental group). ND and HFD are the same values from figure 3.2. All data were compared using a one-way ANOVA with Tukey Post-Hoc and expressed as means ±SEM. Significance was determined at *$p<0.05$, **$p<0.01$. Black solid circle, ND mice; black solid square, HFD mice; blue open circle, ND+iNAC mice; red open square, HFD+iNAC mice. iNAC, intervention study.

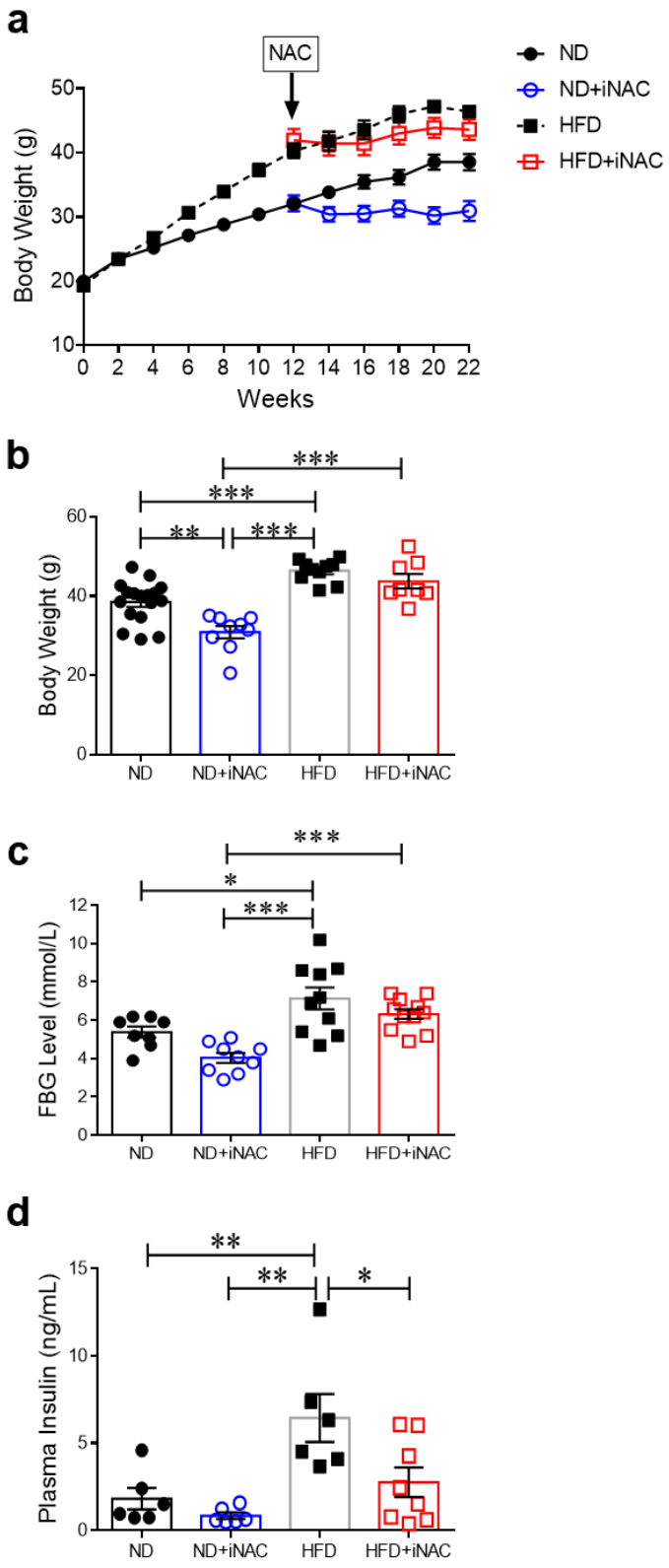
a
NAC
ND
ND+iNAC
HFD
HFD+iNAC
Body Weight (g)
Weeks
b
Body Weight (g)
c
FBG Level (mmol/L)
d
Plasma Insulin (ng/mL)
ND
ND+iNAC
HFD
HFD+iNAC

Figure 3.13

Figure 3.14 NAC intervention treatment for 22 weeks did not restore glucose tolerance in HFD–fed mice.

(a) IPGTT from ND, ND+iNAC, HFD, and HFD+iNAC mice after 22 weeks and (b) area under curve (AUC) analysis of IPGTT. (*n=8-11* mice per experimental group). (c) IPITT from ND, ND+iNAC, HFD, and HFD+iNAC mice after 22 weeks and (d) AUC analysis of IPITT. (*n=5-8* mice per experimental group). ND and HFD are the same values from figure 3.2. All data were compared using a one-way ANOVA with Tukey Post-Hoc and expressed as means ±SEM. Significance was determined at *$p<0.05$, **$p<0.01$. Black solid circle, ND mice; black solid square, HFD mice; blue open circle, ND+iNAC mice; red open square, HFD+iNAC mice. iNAC, intervention study.

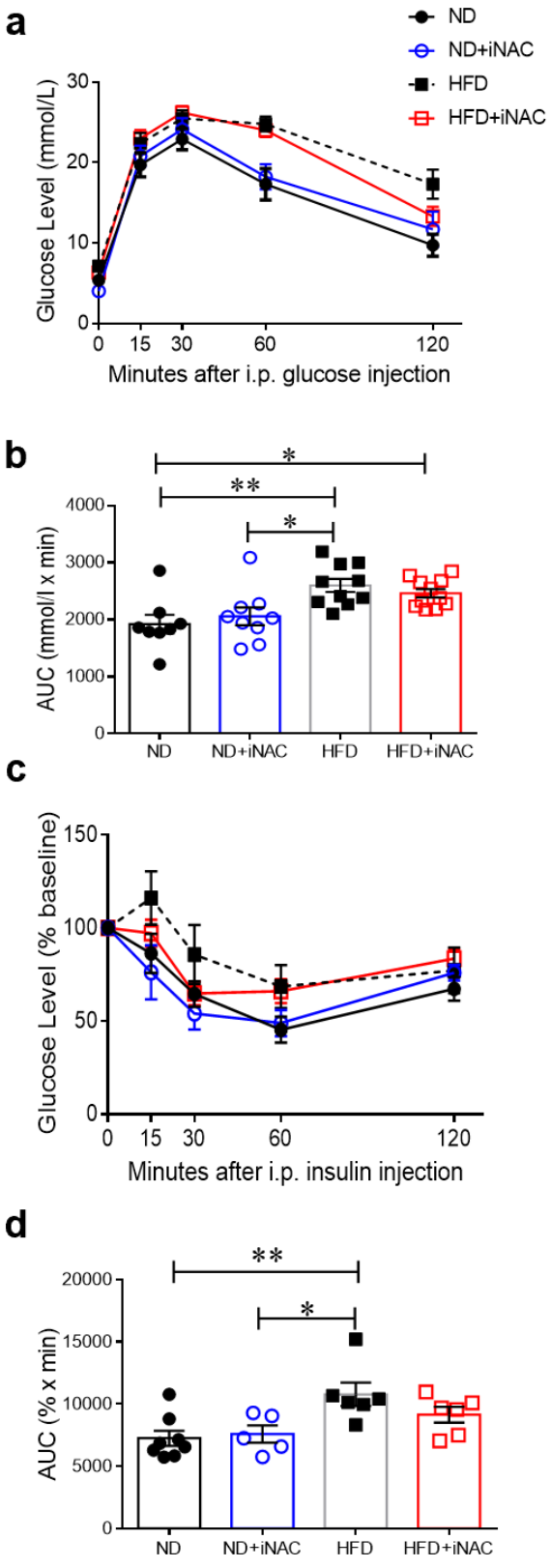
a
ND
ND+iNAC
HFD
HFD+iNAC
Glucose Level (mmol/L)
30
20
10
0
0 15 30 60 120
Minutes after i.p. glucose injection
b
*
**
*
AUC (mmol/l x min)
4000
3000
2000
1000
0
ND
ND+iNAC
HFD
HFD+iNAC
c
Glucose Level (% baseline)
150
100
50
0
0 15 30 60 120
Minutes after i.p. insulin injection
d
**
*
AUC (% x min)
20000
15000
10000
5000
0
ND
ND+iNAC
HFD
HFD+iNAC

Figure 3.14

3.7 Intervention NAC treatment affected islet morphology in 22-week ND and HFD mice

Morphological analysis for islet density showed no significantly altered islet number in the pancreatic sections between experimental groups (Figure 3.15a). Increased beta cell mass was found in HFD mice compared to ND mice after 22 weeks study with similar alpha cell mass observed (Figure 3.15b and 15c). Similar beta and alpha cell mass were observed between the ND and ND+iNAC mouse pancreas. However, HFD-induced increased beta cell mass was reduced in HFD+iNAC mice (Figure 3.15b and 15c). However, this did not reach statistical significance as variability was noted between HFD and HFD+iNAC groups.

To verify whether reduced beta cell mass was associated with the beta cell size and number, individual beta cell size and total number of beta cells in the islets was measured. Significantly larger beta cell size with lower beta cell number in the islets was found in the HFD mice compared to ND mice, with no change in the size and the number between ND and ND+iNAC groups (Figure 3.16). However, HFD+iNAC mice displayed significantly smaller beta cell size and higher beta cell number in islets when compared to HFD mice (Figure 3.16). Both beta cell size and number in HFD+iNAC mice were similar to ND and ND+iNAC groups, suggesting HFD mice under intervention NAC treatment could restore a normal beta cell phenotype seen in ND mice.

Figure 3.15 Intervention NAC treatment affected islet morphology in ND and HFD at 22 weeks.

(a) The number of islets in the pancreas of all experimental groups at 22 weeks of diet with NAC intervention. (*n=3-5* mice per experimental group). Morphometric quantification of (b) beta and (c) alpha cell mass of all experimental groups. (*n=3-6* mice per experimental group). ND and HFD beta cell mass and islet density are the same values compared in figure 3.12. All data are compared using one-way ANOVA with Tukey Post-Hoc and expressed as means ±SEM. Black solid circle, ND mice; black solid square, HFD mice; blue open circle, ND+iNAC mice; red open square, HFD+iNAC mice. iNAC, intervention study.

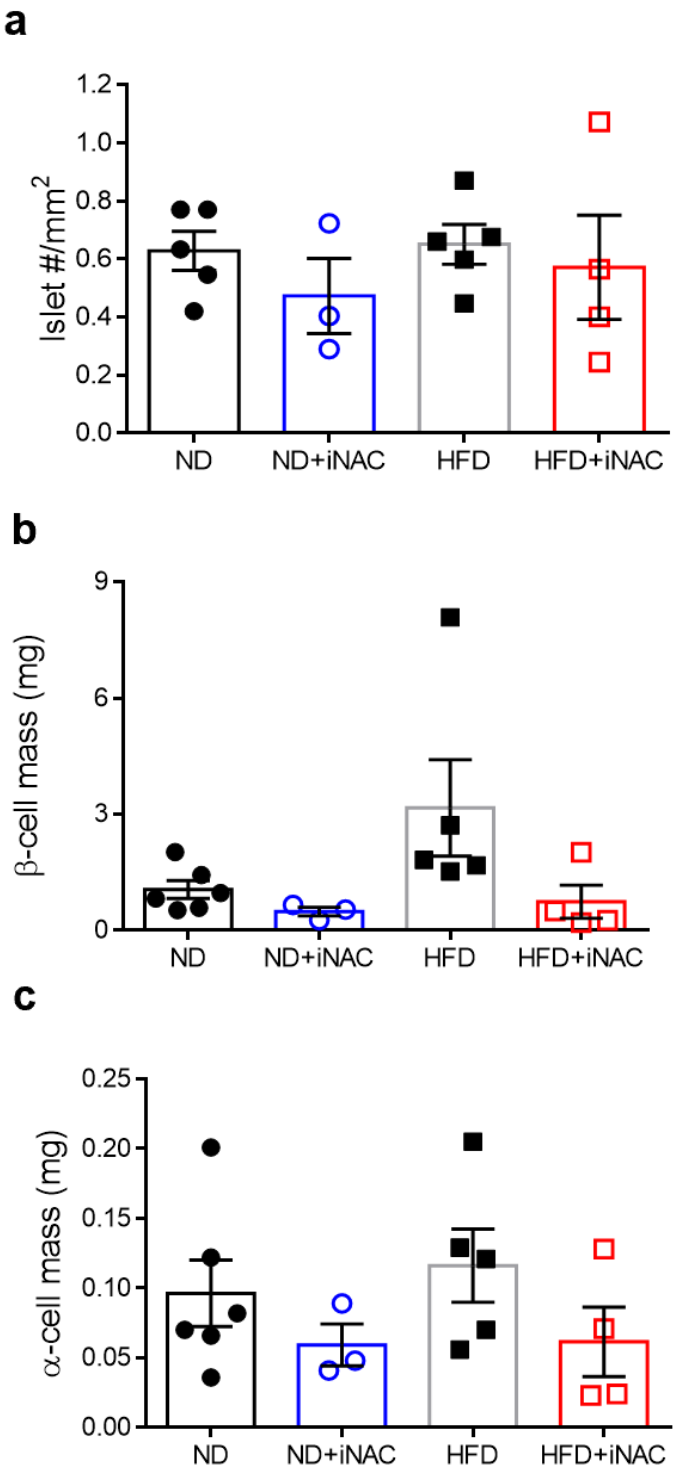
a
Islet #/mm2
1.2
1.0
0.8
0.6
0.4
0.2
0.0
ND
ND+iNAC
HFD
HFD+iNAC
b
β-cell mass (mg)
9
6
3
0
ND
ND+iNAC
HFD
HFD+iNAC
c
α-cell mass (mg)
0.25
0.20
0.15
0.10
0.05
0.00
ND
ND+iNAC
HFD
HFD+iNAC

Figure 3.15

Figure 3.16 Intervention NAC treatment affected beta cell size and number in ND and HFD at 22 weeks.

(a) Average beta cell size and (b) number of beta cells in the insulin^{+} area of ND, ND+iNAC, HFD and HFD+iNAC mice at 22 weeks of diet with NAC intervention. (*n=4-6* mice per experimental group). (c) Representative double immunofluorescence images for glucagon (green) and insulin (red) staining for ND, ND+iNAC, HFD and HFD+iNAC treated pancreata. DAPI, blue. Scale bar, 50 μm. All data were compared using a one-way ANOVA with Tukey Post-Hoc and expressed as means ±SEM. Significance was determined at *$p<0.05$, **$p<0.01$. Black solid circle, ND mice; black solid square, HFD mice; blue open circle, ND+iNAC mice; red open square, HFD+iNAC mice. iNAC, intervention study.

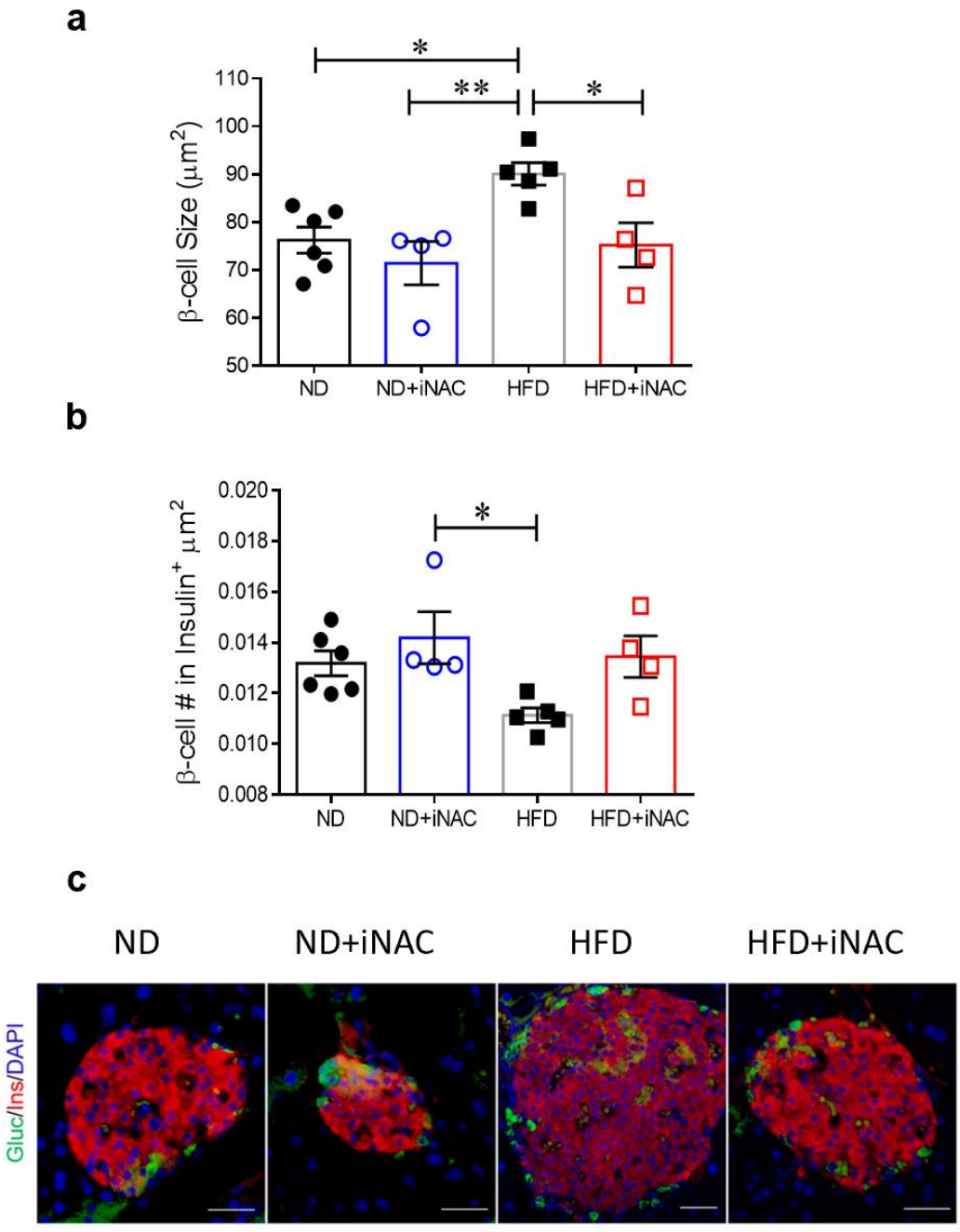
a
β-cell Size (μm²)
110
100
90
80
70
60
50
*
**
*
ND
ND+iNAC
HFD
HFD+iNAC
b
β-cell # in Insulin⁺ μm²
0.020
0.018
0.016
0.014
0.012
0.010
0.008
*
ND
ND+iNAC
HFD
HFD+iNAC
c
ND
ND+iNAC
HFD
HFD+iNAC
Gluc/Ins/DAPI

Figure 3.16

Figure 3.17 Beta-cell proliferation in 22-week ND and HFD mice on a NAC intervention treatment.

(a) Representative double immunofluorescence images of Ki67 (green) and insulin (red) staining of ND, ND+iNAC, HFD and HFD+iNAC treated pancreata. DAPI, blue. Scale bar, 50 μm. Asterisks represent non-specific blood staining and arrows indicate positive signaling. (b) Percentage of Ki67 and insulin positive co-stained cells over total insulin positive cells to determine beta cell proliferation in the islets of ND mice compared to ND+iNAC mice and HFD mice compared to HFD+iNAC mice. All data were compared using a one-way ANOVA with Tukey Post-Hoc are expressed as means ±SEM (*n= 3-4* mice per experimental group). Black solid circle, ND mice; black solid square, HFD mice; blue open circle, ND+pNAC mice; red open square, HFD+pNAC mice. iNAC, intervention study.

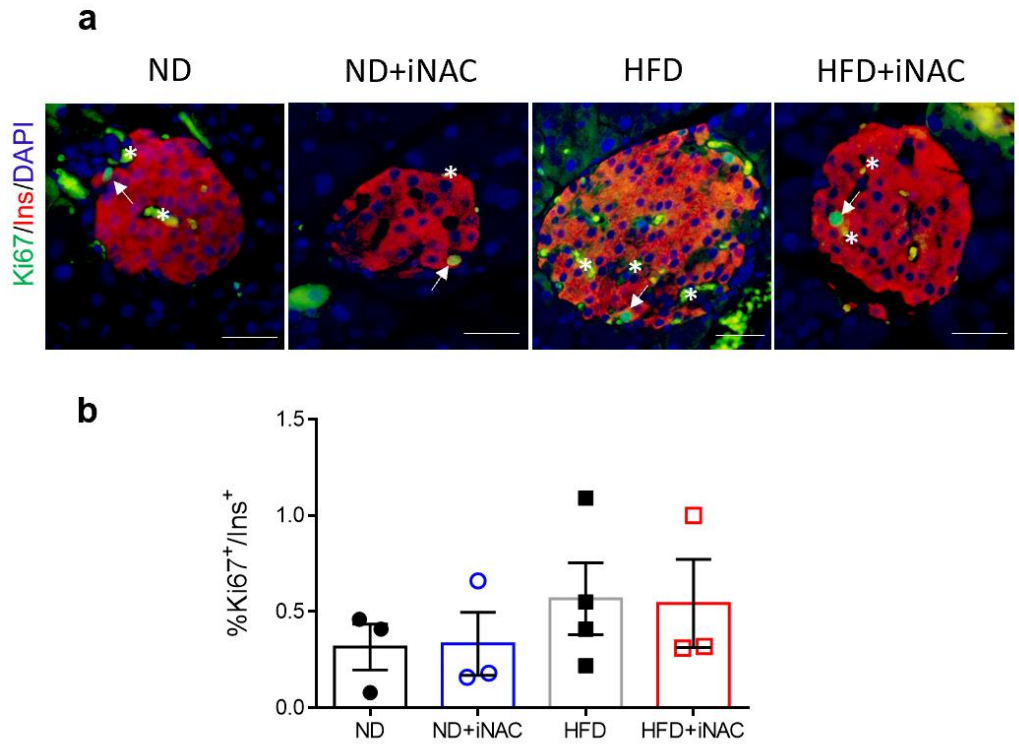
a
ND
ND+iNAC
HFD
HFD+iNAC
Ki67/Ins/DAPI
b
%Ki67+/Ins+
1.5
1.0
0.5
0.0
ND
ND+iNAC
HFD
HFD+iNAC

Figure 3.17

3.8 Intervention NAC treatment restored nuclear PDX-1 expression and lowered intra-islet PaSC activation

To examine whether NAC intervention treatment improved beta cell PDX-1 expression, double immunostaining for PDX-1 with insulin was performed (Figure 3.18a). The nuclear PDX-1 localization in HFD beta cells was significantly reduced compared to ND beta cells after 22 weeks of diet (Figure 3.18b). There was no change in nuclear PDX-1 localization between ND and ND+iNAC groups, but HFD+iNAC beta cells significantly improved of nuclear PDX-1 localization compared to HFD beta cells (Figure 3.18b).

Furthermore, the PaSC activation marker αSMA was increased in islets of HFD mice compared to ND mice (Figure 3.19a), as determined by double immunofluorescence staining for αSMA and insulin (Figure 3.19b). Similar activation levels of PaSCs were observed between ND and ND+iNAC groups, but PaSCs populations were reduced in HFD+iNAC islets when compared to HFD (Figure 3.19c).

Figure 3.18 Intervention NAC treatment affected beta cell PDX-1 expression under ND and HFD at 22 weeks.

(a) Representative double immunofluorescence images for PDX-1 (green) and insulin (red) staining for ND, ND+iNAC, HFD and HFD+iNAC mouse pancreata with PDX-1 (green) images only below each representative. DAPI, blue. Scale bar, 50 μm. (b) The percent of nuclear PDX-1 staining found in the beta cells of ND, ND+iNAC, HFD and HFD+iNAC mice. (*n=4* mice per experimental group). DAPI, blue. Scale bar, 50 μm. All data were compared using a one-way ANOVA with Tukey Post-Hoc and expressed as means ±SEM. Significance was determined at *$p<0.05$, **$p<0.01$. Black solid circle, ND mice; black solid square, HFD mice; blue open circle, ND+iNAC mice; red open square, HFD+iNAC mice. iNAC, intervention study.

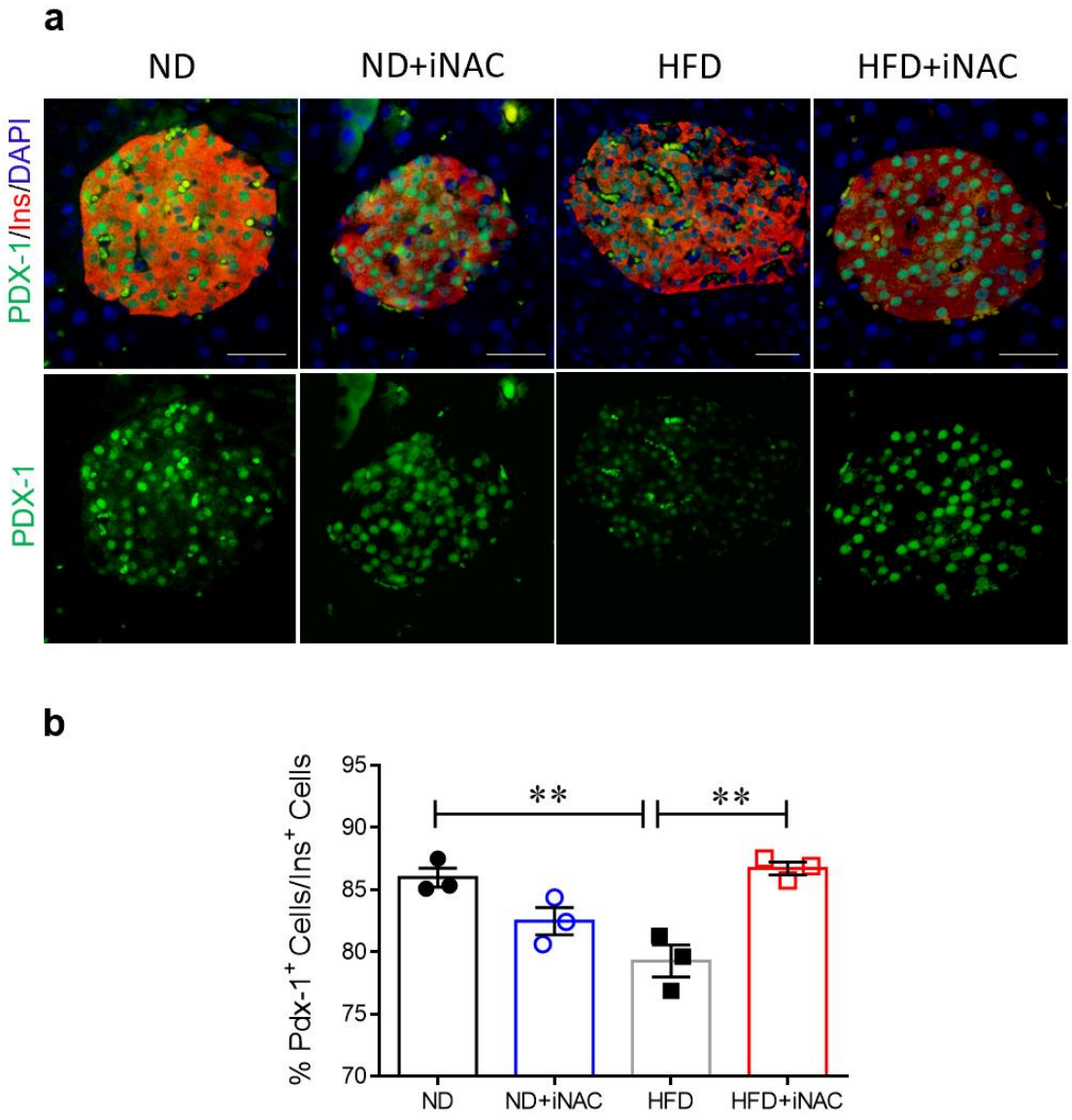
a
ND
ND+iNAC
HFD
HFD+iNAC
PDX-1/Ins/DAPI
PDX-1
b
% Pdx-1+ Cells/Ins+ Cells
95
90
85
80
75
70
**
**
ND
ND+iNAC
HFD
HFD+iNAC

Figure 3.18

Figure 3.19 Intervention NAC treatment affected the islet PaSC population under ND and HFD at 22 weeks.

(a) Quantitative analysis of activated PaSCs, labeled by αSMA, in the islets of ND, ND+iNAC, HFD and HFD+iNAC groups. (b) Representative double immunofluorescence images for αSMA (green) with insulin (red) (*n=4-5* mice per experimental group) with αSMA (green) channels alone beneath each representative and DAPI, blue. Scale bar, 50 μm. (*n=3* mice per experimental group). All data were compared using a one-way ANOVA with Tukey Post-Hoc and expressed as means ±SEM. Black solid circle, ND mice; black solid square, HFD mice; blue open circle, ND+iNAC mice; red open square, HFD+iNAC mice. iNAC, intervention study.

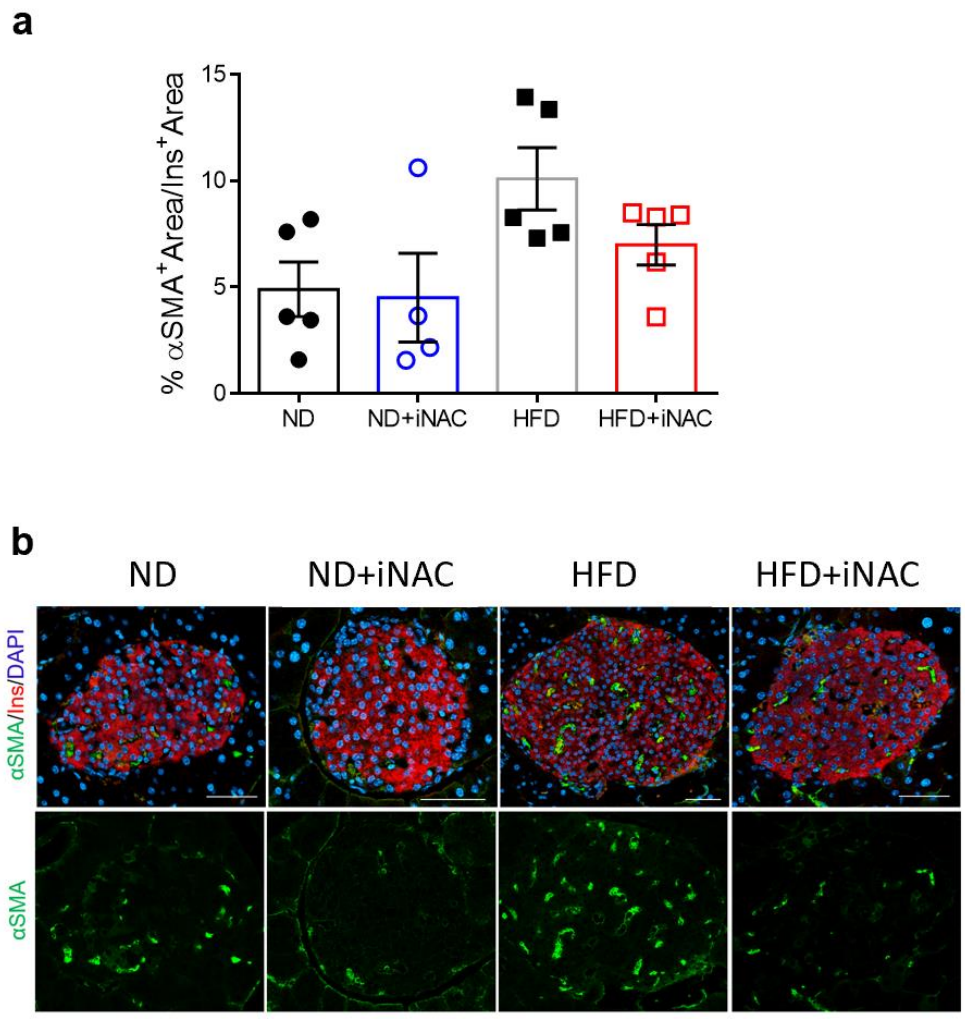
a
% αSMA+Area/Ins+Area
15
10
5
0
ND
ND+iNAC
HFD
HFD+iNAC
b
ND
ND+iNAC
HFD
HFD+iNAC
αSMA/Ins/DAPI
αSMA

Figure 3.19

Chapter 4

4 Discussion

The objective of this study was to determine the effects of NAC treatment on beta cell function under normal or high fat diet condition when administered as either a preventative or intervention treatment. It was hypothesized that preventing HFD-induced beta cell dysfunction using NAC will improve beta cell function and reduce the activation of the islet PaSC (αSMA^+) population. B6N mice were fed a short-term (8 weeks) or long-term (22 weeks) 60% HFD to determine the onset of glucose intolerance before application of preventative NAC (throughout 8- or 22-week HFD) or intervention NAC (beginning at week 12 of a 22-week HFD) treatments. The findings from this thesis demonstrated that an 8-week preventative NAC treatment did not induce metabolic and histologic effects on glucose tolerance and islet morphology but did reduce the presence of αSMA^+ cells within HFD islets. Long-term NAC prevention treatment improved glucose tolerance and insulin sensitivity by reducing weight gain in HFD mice. However, NAC intervention prevented compensatory beta cell hypertrophy and restored PDX-1 localization but did not restore glucose tolerance in HFD mice. The aims from this study helped elucidate the effectiveness of NAC on metabolic outcomes when applied at different times during T2DM progression and the effects NAC exerts on the beta cells at these time points during a prevention or intervention study.

4.1 What duration of HFD is required to induce glucose intolerance and insulin resistance?

B6N mice are commonly used as DIO rodent models of T2DM as they progress through a series of stages similar to what is found in humans (Ingvorsen, Karp, & Lelliott, 2017). Following a 60% HFD for 8 weeks, B6N mice displayed a significant increase in body weight accompanied by glucose intolerance with no significant change to fasting blood glucose (FBG) and insulin tolerance. This is consistent with the findings of Mosser et al. that suggest that changes in glucose metabolism are prior to the existence of insulin resistance in diet-induced obese rodent models (Mosser et al., 2015; Nicholson et al., 2010). In human T2DM, an intermediate stage of prediabetes is described with the

presence of glucose intolerance and/or elevated FBG that are not accompanied by insulin resistance or severe symptoms such as polyuria and polydipsia (Assoc, 2011). An 8-week HFD treatment appears to produce a similar stage of early prediabetes in B6N mice due to the presence of glucose intolerance and lack of additional T2DM signs.

A more severe phenotype emerged after 22-weeks of HFD treatment, which was confirmed by both severely impaired insulin tolerance as well as increased levels of circulating plasma insulin. This was also supported by picrosirius red staining of liver sections in HFD mice compared to ND mice, wherein increased steatosis can be suggestive of impaired organ function (Appendix C) and involved in the progression of insulin resistance (Falach-Malik et al., 2016). Glucose tolerance was worsened at this time when compared to mice on 8 weeks of HFD, and the increase in final body weight of HFD mice compared to ND mice was more pronounced. After 8-weeks of HFD treatment mice presented characteristics of prediabetes but had not progressed to signs of insulin deficiency, which suggested that at 22 weeks HFD mice were more severely glucose impaired than HFD mice at week 8 but had not progressed to uncontrolled hyperglycemic levels (Assoc, 2011; Fisher-Wellman et al., 2016; Rendina-Ruedy et al., 2015). This is consistent with the classification of the DIO B6N mouse model as a model of prediabetes (Rendina-Ruedy et al., 2015).

4.2 Does administration of NAC prior to the beginning of HFD prevent glucose intolerance?

While glucose intolerance was evident at week 8 of HFD in B6N mice, it was not prevented with NAC administration in HFD+pNAC in 8 weeks mice. These mice displayed attenuated weight gain starting at week 6 of HFD compared to HFD only mice and displayed a slight improvement in insulin sensitivity from 0-30 minutes post-injection. However, final body weight and insulin tolerance after 8 weeks of diet in HFD+pNAC and HFD mice were not significant. While other studies have found a significant improvement in glucose tolerance in B6J mice following a 9-week HFD with 400 mg/kg/day of NAC in drinking water, these mice also had a significant reduction in body weight that was unrelated to alterations in food consumption (Falach-Malik et al., 2016). It has long been known that body weight reduction is able to improve glucose

tolerance and insulin sensitivity (Hamman et al., 2006). Mice of a B6J background gained weight at different rates than those with a B6N background (Fisher-Wellman et al., 2016; Nicholson et al., 2010) which may account for changes in the length of time required to achieve weight loss for our B6N mice treated with NAC. It appears that weight loss independent of reduced food consumption played a role in the outcomes associated with NAC. Alterations may be occurring with insulin sensitivity in 8-week prevention HFD+pNAC mice but may not have reached significance as significant changes to HFD mice compared to ND mice had not yet developed. Therefore, the continuation of NAC administration with diet for a longer time period may have produced more conclusive improvements to glucose tolerance.

Previous studies have suggested that longer treatment periods with NAC increased its effectiveness and induced weight loss in rodents (Shen et al., 2019). To determine whether improvements could be found following a long-term preventative treatment with NAC, mice were treated with pNAC for a duration of 22 weeks. Following HFD+pNAC for 22 weeks, these mice displayed significantly improved glucose tolerance and improved FBG compared to 22-week HFD mice. Significantly improved insulin tolerance as well as reduced circulating plasma insulin levels were also noted. Studies involving NAC administration often demonstrate increased effectiveness when decreased body weight is independent of reduced caloric intake (Falach-Malik et al., 2016; Novelli et al., 2009; Shen et al., 2019). Consistent with these findings, the increased effectiveness of NAC on metabolic outcomes found in HFD+pNAC mice following during a 22-week HFD were associated with a reduction in weight gain, independent of reduced caloric intake. While caloric intake is not responsible for alterations in weight gain, Novelli et al. and Shen et al. have suggested increased motor activity and changes to metabolic activity levels which may account for the changes to weight gain on HFD+pNAC (Novelli et al., 2009; Shen et al., 2019).

4.3 Does preventative NAC administration enhance beta cell mass during early compensation in HFD mice?

During oxidative stress, beta cells are known to increase beta cell mass predominantly through proliferation, which is one of the first changes made in the beta cell population in response to HFD (Mosser et al., 2015). When oxidative stress is reduced through antioxidant such as NAC, it has been suggested that beta cells decrease proliferation (Alfar et al., 2017). Mice fed HFD for 8 weeks did not display increased beta cell mass compared to ND but displayed increasing proliferation rates. However, beta cell mass in appeared relatively unchanged in HFD+pNAC mice compared to HFD-fed mice for 8 weeks. Interestingly, ND+pNAC mice displayed a trend towards decreased beta cell mass compared to ND mice following 8-weeks of diet, which was accompanied by a decrease in alpha cell mass. This may be due to a reduction in the number of islets found per mm^2. Alfar et al. have found a physiological role of H_2O_2 in beta cell proliferation, which is inhibited by antioxidants such as NAC (Alfar et al., 2017) and may account for the reduction in ND+pNAC beta cell mass during a potential time of physiological expansion.

The 8-week time point has shown to be an early time point in T2DM progression, leading to the evaluation of beta cell mass following NAC prevention 1 week prior to and during 22 weeks of diet. Following an increase in beta cell mass in HFD islets compared to ND, long term NAC prevention did not alter beta cell mass in long term ND+pNAC samples but normalized beta cell mass in HFD+pNAC pancreata. These changes were unrelated to changes in total islet number. Taken with the improved metabolic testing, long-term NAC prevention may be protecting the beta cells from markers related to over-compensatory related dysfunction seen at this time point. More studies on the cause behind a lack of HFD induced beta cell mass increase following long term NAC prevention are warranted to determine whether the lack of increase is due to alterations in size or proliferation rates. Additionally, whether long-term pNAC is effective at not only restoring normal beta cell mass, but also markers of function will be examined in future studies. Interestingly, a large reduction in αSMA^+ area indicative of PaSC activation was found in HFD+pNAC compared to HFD islets at 22 weeks of diet. A lack of PaSC activation and

associated growth factors could be partially responsible for the lack of increased beta cell mass at this time point.

4.4 Is preventative NAC treatment able to inhibit the activation of PaSCs *in vivo*?

Active PaSCs are identified *in vivo* primarily through the marker αSMA. Intra-islet immunofluorescence staining showed an increase in αSMA^+ cell area in the islets of 8-week HFD mice compared to ND mice and this was reduced in HFD+pNAC mice. Intra-islet αSMA+ area in the islets of 22-week HFD mice was also increased compared to ND mice, which was greatly reduced by long term NAC prevention treatment, suggesting that once NAC is administered it is able to prevent as well as maintain low levels of intra-islet PaSC activation. Whether a lack of PaSC associated growth factors is partially responsible for the decreased beta cell mass found in 22-week HFD+pNAC mice has yet to be determined and will be examined in future studies.

Antioxidants such as NAC have been shown to decrease PaSC activation (Asaumi et al., 2007; Jesnowski et al., 2005) *in vitro* in primary cultured PaSCs, while antioxidants such as pirfenidone have been shown to reduce intra-islet activation *in vivo* (Lee et al., 2017). Whether the inhibition of PaSC activation prior to and during HFD contributes to alterations in beta cell function in a beneficial or negative manner has yet to be elucidated.

4.5 Does administration of NAC during HFD improve glucose tolerance?

A severe prediabetic state, including severely impaired glucose tolerance found following 22 weeks of HFD, was not significantly improved with HFD+iNAC treatment. Significantly improved circulating plasma insulin level suggestive of improved hyperinsulinemia was found compared to HFD. However, only a mild improvement in insulin tolerance was observed through a lack of significant improvement between HFD and HFD+iNAC groups, but the loss of significant difference between ND and HFD+iNAC found following intervention treatment. Improved liver steatosis in HFD+iNAC mice compared to HFD mice were also noted, suggesting improvements that

may have affected peripheral insulin resistance (Appendix C). Interestingly, glucose tolerance from 0-60 minutes was not improved, while glucose levels in HFD+iNAC mice appeared to return closer to baseline levels compared to HFD mice at 120 minutes. It has been suggested that the first phase of insulin release is sometimes more severely impacted by T2DM progression (Pedersen et al., 2019), which leaves the possibility that the second phase of insulin release may be improved first during iNAC treatment while the first, more heavily impacted phase may require more treatment time. As with pNAC treatment for 8 weeks, iNAC mice did not display significantly reduced final body weight but showed a pattern of mild body weight gain attenuation following the start of NAC treatment. This was not related to caloric intake, in which there was no reduction. B6J mice have been shown to display significantly improved insulin resistance and glucose tolerance when put on NAC intervention treatment beginning at month 3 during a 6-month HFD. While these mice did not lose a significant amount of body weight at 6 months, the study showed improved glucose tolerance and insulin tolerance in mice given NAC from 1-6 months of HFD compared to 3-6 months of HFD, supporting the importance of a long-term treatment time in the effectiveness of NAC (Shen et al., 2019). Additionally, it is important to note the changes in the background of the mice in which the study was conducted. B6N and B6J mice gain weight at different rates, and motor activity is affected differently in each strain which may account for the differences in rate of weight gain (Nicholson et al., 2010). Mice in the current study appear to be at the beginning of metabolic improvements, and it is conceivable that the extra month of NAC treatment afforded to the HFD+iNAC mice in the Shen et al. study would allow for improvements in metabolic outcomes.

In ND+iNAC mice, a significant reduction in final body weight was noted that was associated with a reduction in FBG, while caloric intake was unchanged. Studies have suggested that NAC is able to alter metabolic activity levels to cause weight loss that is not caused by a decrease in caloric intake (Novelli et al., 2009; Shen et al., 2019), which may account for alterations to ND metabolic outcomes following treatment with NAC.

4.6 Does administration of NAC during HFD prevent later stage beta cell failure associated with T2DM progression?

Progression of beta cells through T2DM-like DIO involves compensation, dysfunction, and eventual failure. Compensation is characterized by an increase in mass due to increased proliferation and/or size (Alfar et al., 2017; Granot et al., 2009) which contributes to hyperinsulinemia. Following a 22-week HFD, an increase in beta cell mass associated with the compensatory stage was found when compared to ND mice. Beta cells in the HFD environment increased in size and proliferation rates compared to ND in order to increase mass as well as insulin production. It was found that HFD+iNAC beta cell size was significantly smaller than in HFD mice, reflecting a size more comparable to that found in ND mice. HFD+iNAC normalized overall beta cell mass, an improvement compared to the increased beta cell mass found in HFD. These changes were unrelated to changes in beta cell proliferation rates. However, with the current lack of change in proliferation rates, it is not clear whether a change of mass at this time point is attenuated or reversed. While HFD mice display markers of compensation in response to HFD, it appears that HFD+iNAC reduces mechanisms indicative of over-compensation leading to hyperinsulinemia.

In addition to markers of compensation, HFD beta cells at 22 weeks displayed signs of dysfunction. Nuclear PDX-1 localization is responsible for inducing insulin transcription, thereby maintaining overall insulin levels within the beta cells and is indicative of beta cell identity (Kawamori et al., 2003; Ma et al., 2016). A significant reduction in nuclear PDX-1 localization was found in the beta cells of HFD mice compared to ND mice and is a classic sign of dysfunction related to oxidative stress (Kawamori et al., 2003). NAC has been shown to improve nuclear PDX-1 mRNA levels in islets isolated from ZDF rats (Tanaka et al., 1999). Consistent with these findings HFD+iNAC beta cells displayed significantly improved nuclear PDX-1 localization compared to HFD islets, suggesting either a reversed or delayed dysfunctional state in relation to insulin production.

4.7 Is intervention NAC treatment able to reduce PaSC activation during HFD *in vivo*?

n Increased in intra-islet αSMA+ staining in 22-week HFD islets compared to ND islets was reduced in HFD+iNAC islets compared to HFD, suggesting a reduction in PaSC activation. Once PaSCs are initially activated by factors such as ROS, they continue activation through autocrine and paracrine factors (Saito et al., 2012). While difficult to reduce or reverse PaSC activation, it has been found that NAC is capable of deactivating PaSCs *in vitro* under the correct environmental conditions (Jesnowski et al., 2005). PaSCs are capable of producing growth factors and hormones (Ryu et al., 2013) that may be involved in the HFD-induced increase of beta cell mass that is absent following iNAC treatment at this time point. Whether reducing intra-islet PaSC activation has a positive or negative influence on this stage of compensation has yet to be determined.

4.8 Limitations of the Study and Methodology

The DIO B6N model has many benefits, including less genetic drift and the presence of the wildtype *Nnt* gene, which is also present in humans (Fisher-Wellman et al., 2016). However, this model is generally accepted as a prediabetic model in T2DM progression (Rendina-Ruedy et al., 2015), which does not typically progress to overt diabetes characterized by weight loss and loss of beta cell mass. Without such markers of dysfunction, it is difficult to determine the effects of NAC on attenuation versus prevention on dysfunction as the model likely will not progress to this severe T2DM state (King, 2012). However, finding a DIO model that progresses past prediabetes without the presence of genetic manipulation is challenging and would introduce a confounding variable in the assessment of the effects of an antioxidant on beta cell compensation and dysfunction. While wild type HFD DIO mouse models are accepted models displaying the importance of oxidative stress in the beginning of and during T2DM progression, the use of alternative mouse models may be necessary to more effectively determine the late stage effects of NAC treatment on beta cell function.

Studies suggest alterations in motor activity or genes related to motor activity can lead to reduced body weight without reduced caloric intake (Novelli et al., 2009; Shen et al.,

2019). While it was determined that a reduction of caloric intake was not the cause of reduced body weight in ND mice treated with NAC in the short-term prevention and intervention studies, motor studies and genetic analysis were not performed to determine whether alterations in motor activity was the cause of weight gain attenuation. It is important to note no stimuli were added in the cages that could differentially impact exercise levels compared to other studies and no caloric intake alterations were found in ND compared to ND+NAC mice, suggesting that motor activity and related genes should be examined in B6N mice and compared to the changes found in B6J mice to determine whether these are the definitive causes of weight gain attenuation.

A major limitation of assessing PaSC activation is a lack of the existence of specific markers to determine active PaSCs from intra-islet pericytes. However, pericytes and PaSCs likely belong to the same family of mesenchymal-like cells that exist within the islet, with the difference between the two types being that pericytes have been shown to exist surrounding vessels (Erkan et al., 2012). Additionally, Hayden et al. have suggested that pericytes may be able to differentiate into PaSCs (Hayden et al., 2007). However, one suggested marker that is not shared between pericytes and PaSCs may be Nkx3.2 (Sasson et al., 2016). With this topic still largely under debate, αSMA^+ positive cells are considered suggestive of PaSC activation for the purposes of this study. Lastly, when staining for αSMA^+ area, a mouse derived antibody was used on mouse tissue which leaves the opportunity for the anti-mouse secondaries to bind to non-specific antigens within the tissue resulting in high background. When quantifying, only positive αSMA^+ area with distinct cytoplasmic staining around a nucleus was counted. However, as mouse on mouse staining does result in higher background either a rabbit derived αSMA antibody or a mouse on mouse kit should be considered in the future.

Lastly, large variability due to low sample sizes was observed in assays of 8-week NAC prevention samples. This sample size will be increased in future studies.

4.9 Conclusion and Future Direction

In summary, this study suggests that NAC is most effective on overall metabolic outcomes when administered for a treatment period long enough to induce significant

weight gain attenuation. While 8 weeks appears to be too early to see the full effect of prediabetes induced by HFD, pNAC at this time point can improve beta cell proliferation rates as well as decrease intra-islet αSMA^+ staining. Following intervention treatment, NAC partially protects beta cells from signs of overcompensation as well as dysfunction that are associated with a long-term HFD, while reducing intra-islet αSMA^+ staining.

To determine whether dysfunction at later stages was attenuated, prevented, or reversed markers for apoptosis, such as caspase-3 (Porter & Jänicke, 1999) must be examined in the *in vivo* embedded samples. Additionally, a mouse model reliant on oxidative stress driving T2DM progression to dysfunction should be utilized in order to determine the effective NAC at protecting beta cell viability. One such model that must be considered is the streptozotocin (STZ)/HFD rat model. T2DM may be induced in this model with multiple, smaller doses of STZ compared to the dosage required to induce T1DM. STZ is a beta cell toxin, and when paired with HFD to induce hyperinsulinemia, insulin resistance and hyperglycemia allow for both early and late stages of T2DM to be examined as opposed to the prediabetic model produced by HFD alone (Skovsø, 2014). Using the STZ/HFD model to induce both early and late stages of T2DM and applying a long-term prevention or intervention NAC treatment could shed light on whether the effects of NAC are causing attenuation or reversal of dysfunction in the beta cells.

While NAC is a well-known antioxidant, it is important to determine how effective the drug is at reducing levels of oxidative stress within the islets at the various treatment times and at the specific dosages used within the study. While NAC is likely more effective at the higher dosage because it reduces oxidative stress more so than a lower dosage, this must be confirmed using immunohistochemical markers of intra-islet ROS levels such as 8-hydroxy-2’-deoxyguanosine (8-OHdG) (Miki et al., 2018).

Lastly, while NAC appears to be protecting beta cell function from DIO induced dysfunction, how it is exerting its effects has yet to be determined. Whether NAC is affecting beta cell function directly or indirectly is a long-standing question. This study demonstrates a reduction of intra-islet PaSC activation, which can be related to alterations in beta cell mass and function at various points throughout T2DM progression.

Whether NAC exerts a direct effect, an indirect effect, or potentially both through the subsequent effects of PaSC reduction have yet to be determined. To help determine whether NAC exerts primarily direct or indirect effects, administration of NAC on islets isolated from ND and HFD mice following 22 weeks of diet to assess its direct antioxidant capacity compared to glutathione administration to assess indirect antioxidant effects should be conducted. Additionally, a similar assay should be conducted on isolated PaSCs from 22-week ND or HFD mice to determine whether NAC has an indirect or direct effect on PaSC activation levels. Additionally, while a co-culture of isolated islets and PaSCs have shown to have an overall negative effect on insulin production within the beta cells (Zang et al., 2015), it is not known if the reduction of PaSC activation plays positive or negative roles in beta cell viability at the various stages, and how those effects may be employed provide a future avenue for NAC and beta cell related studies. To potentially assess the effects of PaSCs on beta cell viability, PaSCs isolated from NAC treated or non-treated mice following an intervention or long-term prevention study should be either directly cultured with islets isolated from age-matched mice or cultured via a transwell system. It is difficult to study PaSCs *in vitro* due to their ability to become activated by the culture plate and process, but it has been suggested that this activation may be attenuated using Matrigel (Jesnowski et al., 2005). Utilizing these methods could help determine the role of PaSCs on beta cell function at various time points during T2DM progression in a diet-induced obesity model.

References

Ahlgren, U., Jonsson, J., Jonsson, L., Simu, K., & Helena, E. (1998). Beta-Cell-specific inactivation of the mouse Ipf1/Pdx1 gene results in loss of the beta-cell phenotype and maturity onset diabetes. *Genes and Development*, *12*, 1763–1768. Retrieved from https://www-ncbi-nlm-nih-gov.proxy1.lib.uwo.ca/pmc/articles/PMC316911/pdf/x5.pdf

Alfar, E. A., Kirova, D., Konantz, J., Birke, S., Mansfeld, J., & Ninov, N. (2017). Distinct Levels of Reactive Oxygen Species Coordinate Metabolic Activity with Beta-cell Mass Plasticity. *Scientific Reports*, *7*(1), 3994. https://doi.org/10.1038/s41598-017-03873-9

Apte, M. V, Haber, P. S., Applegate, T. L., Norton, I. D., McCaughan, G. W., Korsten, M. A., … Wilson, J. S. (1998). Periacinar stellate shaped cells in rat pancreas: identification, isolation, and culture. *Gut*, *43*(1), 128–133. Retrieved from http://www.ncbi.nlm.nih.gov/pubmed/9771417

Asaumi, H., Watanabe, S., Taguchi, M., Tashiro, M., & Otsuki, M. (2007). Externally applied pressure activates pancreatic stellate cells through the generation of intracellular reactive oxygen species. *American Journal of Physiology - Gastrointestinal and Liver Physiology*, *293*(5), G972-8. https://doi.org/10.1152/ajpgi.00018.2007

Ashor, A. W., Lara, J., Willis, N. D., Mathers, J. C., & Siervo, M. (2017). Effects of vitamin C supplementation on glycaemic control: a systematic review and meta-analysis of randomised controlled trials. *European Journal of Clinical Nutrition*, *71*, 1371–1380. https://doi.org/10.1038/ejcn.2017.24

Assoc, A. D. (2011). Diagnosis and Classification of Diabetes Mellitus AMERICAN DIABETES ASSOCIATION. *Diabetes Care*, *34*(Supplement 1), S62–S69. https://doi.org/10.2337/dc11-S062

Aston-Mourney, K., Wong, N., Kebede, M., Zraika, S., Balmer, L., McMahon, J. M., … Andrikopoulos, S. (2007). Increased nicotinamide nucleotide transhydrogenase levels predispose to insulin hypersecretion in a mouse strain susceptible to diabetes. *Diabetologia*, *50*(12), 2476–2485. https://doi.org/10.1007/s00125-007-0814-x

Beckman, J. A., Goldfine, A. B., Leopold, J. A., & Creager, M. A. (2016). Ebselen does not improve oxidative stress and vascular function in patients with diabetes: a randomized, crossover trial. *American Journal of Physiology. Heart and Circulatory Physiology*, *311*(6), H1431–H1436. https://doi.org/10.1152/ajpheart.00504.2016

Butler, A. E., Janson, J., Bonner-Weir, S., Ritzel, R., Rizza, R. A., & Butler, P. C. (2003). Beta-cell deficit and increased Beta-cell Apoptosis in Humans With Type 2 Diabetes. *Diabetes*, *52*(1), 102–110. https://doi.org/10.2337/diabetes.52.1.102

Campbell-Thompson, M., Rodriguez-Calvo, T., & Battaglia, M. (2015). Abnormalities of the Exocrine Pancreas in Type 1 Diabetes. *Current Diabetes Reports*. https://doi.org/10.1007/s11892-015-0653-y

Chintinne, M., Stangé, G., Denys, B., Ling, Z., In ’t Veld, P., & Pipeleers, D. (2012). Beta Cell Count Instead of Beta Cell Mass to Assess and Localize Growth in Beta Cell Population following Pancreatic Duct Ligation in Mice. *PLoS ONE*, *7*(8). https://doi.org/10.1371/journal.pone.0043959

Cohen, M. I., Gartner, L. M., Blumenfeld, O. O., & Arias, I. M. (1969). Gamma Glutamyl Transpeptidase: Measurement and Development in Guinea Pig Small Intestine. *Pediatric Research*, *3*(1), 5–10. https://doi.org/10.1203/00006450-196901000-00001

Cox, A. R., Lam, C. J., Rankin, M. M., King, K. A., Chen, P., Martinez, R., … Kushner, J. A. (2016). Extreme obesity induces massive beta cell expansion in mice through self-renewal and does not alter the beta cell lineage. *Diabetologia*, *59*(6), 1231–1241. https://doi.org/10.1007/s00125-016-3922-7

Dasgupta, M., Roy, T. K., Mitra, P. S., Adhikari, S., & Bag, T. (2015). Is N-acetylcysteine a better Insulin Sensitizer than Metformin in Polycystic Ovarian Syndrome. *Andrology and Gynecology: Current Research*, *3*(3).

Dekhuijzen, P. N. R. (2004). Antioxidant properties of N-acetylcysteine: their relevance in relation to chronic obstructive pulmonary disease. *Eur Respir J*, *23*, 629–636. https://doi.org/10.1183/09031936.04.00016804

Dolenšek, J., Rupnik, M. S., & Stožer, A. (2015). Structural similarities and differences between the human and the mouse pancreas. *Islets*. Taylor & Francis. https://doi.org/10.1080/19382014.2015.1024405

Erkan, M., Adler, G., Apte, M. V, Bachem, M. G., Buchholz, M., Detlefsen, S., … Wilson, J. (2012, February). StellaTUM: Current consensus and discussion on pancreatic stellate cell research. *Gut*. BMJ Publishing Group. https://doi.org/10.1136/gutjnl-2011-301220

Falach-Malik, A., Rozenfeld, H., Chetboun, M., Rozenberg, K., Elyasiyan, U., Sampson, S. R., & Rosenzweig, T. (2016). N-Acetyl-L-Cysteine inhibits the development of glucose intolerance and hepatic steatosis in diabetes-prone mice. *Am J Transl Res*, *8*(9), 3744–3756. Retrieved from www.ajtr.org

Feng, Z C, Li, J., Turco, B. A., Riopel, M., Yee, S. P., & Wang, R. (2012). Critical role of c-Kit in beta cell function: Increased insulin secretion and protection against diabetes in a mouse model. *Diabetologia*. https://doi.org/10.1007/s00125-012-2566-5

Feng, Zhi Chao, Popell, A., Li, J., Silverstein, J., Oakie, A., Yee, S. P., & Wang, R. (2015). C-Kit receptor signaling regulates islet vasculature, β-cell survival, and function in vivo. *Diabetes*, *64*(11), 3852–3866. https://doi.org/10.2337/db15-0054

Fergusson, G., Éthier, M., Guévremont, M., Chrétien, C., Attané, C., Joly, E., … Alquier, T. (2014). Defective insulin secretory response to intravenous glucose in C57Bl/6J compared to C57Bl/6N mice. *Molecular Metabolism*, *3*(9), 848–854. https://doi.org/10.1016/j.molmet.2014.09.006

Fisher-Wellman, K. H., Ryan, T. E., Smith, C. D., Gilliam, L. A. A., Lin, C. Te, Reese, L. R., … Neufer, P. D. (2016). A direct comparison of metabolic responses to high-

fat diet in c57bl/6j and c57bl/6nj mice. *Diabetes*, *65*(11), 3249–3261. https://doi.org/10.2337/db16-0291

Fontaine, D. A., & Davis, D. B. (2016). Attention to Background Strain Is Essential for Metabolic Research: C57BL/6 and the International Knockout Mouse Consortium. *Diabetes*, *65*, 25–33. https://doi.org/10.2337/db15-0982

Frei, B., Kim, M. C., & Ames, B. N. (1990). *Ubiquinol-10 is an effective lipid-soluble antioxidant at physiological concentrations (coenzyme Q/lipid peroxidation/a-tocopherol/heart disease). Proc. Nati. Acad. Sci. USA* (Vol. 87). Retrieved from https://www-ncbi-nlm-nih-gov.proxy1.lib.uwo.ca/pmc/articles/PMC54222/pdf/pnas01037-0476.pdf

Fujii, J., Ito, J.-I., Zhang, X., & Kurahashi, T. (2011). Unveiling the roles of the glutathione redox system in vivo by analyzing genetically modified mice. *Journal of Clinical Biochemistry and Nutrition*, *49*(2), 70–78. https://doi.org/10.3164/jcbn.10-138SR

Granot, Z., Swisa, A., Magenheim, J., Stolovich-Rain, M., Fujimoto, W., Manduchi, E., … Dor, Y. (2009). LKB1 Regulates Pancreatic β Cell Size, Polarity, and Function. *Cell Metabolism*, *10*(4), 296–308. https://doi.org/10.1016/j.cmet.2009.08.010

Hamman, R. F., Wing, R. R., Edelstein, S. L., Lachin, J. M., Bray, G. A., Delahanty, L., … Wylie-Rosett, J. (2006). Effect of weight loss with lifestyle intervention on risk of diabetes. *Diabetes Care*, *29*(9), 2102–2107. https://doi.org/10.2337/dc06-0560

Hayden, M. R., Karuparthi, P. R., Habibi, J., Wasekar, C., Lastra, G., Manrique, C., … Sowers, J. R. (2007a). Ultrastructural islet study of early fibrosis in the Ren2 rat model of hypertension. Emerging role of the islet pancreatic pericyte-stellate cell. *JOP : Journal of the Pancreas*, *8*(6), 725–738. Retrieved from http://www.ncbi.nlm.nih.gov/pubmed/17993725

Hayden, M. R., Karuparthi, P. R., Habibi, J., Wasekar, C., Lastra, G., Manrique, C., … Sowers, J. R. (2007b). Ultrastructural Islet Study of Early Fibrosis in the Ren2 Rat Model of Hypertension. Emerging Role of the Islet Pancreatic Pericyte-Stellate Cell. *JOP. J Pancreas (Online) JOP*, *8*(6), 725–738. Retrieved from http://www.joplink.net/prev/200711/200711_03.pdf

Henquin, J. C., Ishiyama, N., Nenquin, M., Ravier, M. A., & Jonas, J. C. (2002). Signals and pools underlying biphasic insulin secretion. In *Diabetes* (Vol. 51). Retrieved from http://diabetes.diabetesjournals.org/content/51/suppl_1/S60.full-text.pdf

Hong, O.-K., Lee, S.-H., Rhee, M., Ko, S.-H., Cho, J.-H., Choi, Y.-H., … Yoon, K.-H. (2007). Hyperglycemia and Hyperinsulinemia Have Additive Effects on Activation and Proliferation of Pancreatic Stellate Cells: Possible Explanation of Islet-specific Fibrosis in Type 2 Diabetes Mellitus. *Journal of Cellular Biochemistry J. Cell. Biochem*, *101*(101), 665–675. https://doi.org/10.1002/jcb.21222

Hou, J. C., Min, L., & Pessin, J. E. (2009). Insulin granule biogenesis, trafficking and exocytosis. *Vitamins and Hormones*, *80*, 473–506. https://doi.org/10.1016/S0083-6729(08)00616-X

Ingvorsen, C., Karp, N. A., & Lelliott, C. J. (2017). The role of sex and body weight on

the metabolic effects of high-fat diet in C57BL/6N mice. *Nutrition & Diabetes*, *7*, 261. https://doi.org/10.1038/nutd.2017.6

Jesnowski, R., Fü Rst, D., Rg Ringel, J., Chen, Y., Schrö Del, A., Rg Kleeff, J., … Lö Hr, M. (2005). Immortalization of pancreatic stellate cells as an in vitro model of pancreatic fibrosis: deactivation is induced by matrigel and N-acetylcysteine. *Laboratory Investigation*, *85*, 1276–1291. https://doi.org/10.1038/labinvest.3700329

Ježek, P., Jabůrek, M., & Plecitá-Hlavatá, L. (2019). Contribution of Oxidative Stress and Impaired Biogenesis of Pancreatic β-Cells to Type 2 Diabetes. *Antioxidants & Redox Signaling*. https://doi.org/10.1089/ars.2018.7656

Kaneto, H., Matsuoka, T.-A., & Lang, F. (2015). Role of Pancreatic Transcription Factors in Maintenance of Mature β-Cell Function. *Int. J. Mol. Sci*, *16*, 6281–6297. https://doi.org/10.3390/ijms16036281

Kawamori, D., Kajimoto, Y., Kaneto, H., Umayahara, Y., Fujitani, Y., Miyatsuka, T., … Hori, M. (2003). Oxidative stress induces nucleo-cytoplasmic translocation of pancreatic transcription factor PDX-1 through activation of c-Jun NH(2)-terminal kinase. *Diabetes*. Retrieved from http://diabetes.diabetesjournals.org/content/52/12/2896.full-text.pdf

Keane, K. N., Cruzat, V. F., Carlessi, R., De Bittencourt, P. I. H., & Newsholme, P. (2015). Molecular Events Linking Oxidative Stress and Inflammation to Insulin Resistance and β-Cell Dysfunction. *Oxidative Medicine and Cellular Longevity*. Hindawi. https://doi.org/10.1155/2015/181643

Kikuta, K., Masamune, A., Hamada, S., Takikawa, T., Nakano, E., & Shimosegawa, T. (2013). Pancreatic stellate cells reduce insulin expression and induce apoptosis in pancreatic Î²-cells. *Biochemical and Biophysical Research Communications*, *433*, 292–297. https://doi.org/10.1016/j.bbrc.2013.02.095

King, A. J. (2012). The use of animal models in diabetes research Keywords type 1 diabetes; type 2 diabetes; animal models. *British Journal of Pharmacology*, *166*(3), 877–894. https://doi.org/10.1111/(ISSN)1476-5381/homepage/animal_models.htm

Kobayashi, M., Kikuchi, O., Sasaki, T., Kim, H.-J., Yokota-Hashimoto, H., Lee, Y.-S., … Y-s, L. (2012). FoxO1 as a double-edged sword in the pancreas: analysis of pancreas-and-cell-specific FoxO1 knockout mice. *Am J Physiol Endocrinol Metab*, *302*, 603–613. https://doi.org/10.1152/ajpendo.00469.2011.-Dia

Lasram, M. M., Dhouib, I. B., Annabi, A., El Fazaa, S., & Gharbi, N. (2015). A review on the possible molecular mechanism of action of N-acetylcysteine against insulin resistance and type-2 diabetes development. *Clinical Biochemistry*, *48*(16–17), 1200–1208. https://doi.org/10.1016/j.clinbiochem.2015.04.017

Lee, E., Ryu, G. R., Ko, S.-H., Ahn, Y.-B., & Song, K.-H. (2017a). A role of pancreatic stellate cells in islet fibrosis and β-cell dysfunction in type 2 diabetes mellitus. *Biochemical and Biophysical Research Communications*, *485*(2), 328–334. https://doi.org/10.1016/J.BBRC.2017.02.082

Lee, E., Ryu, G. R., Ko, S. H., Ahn, Y. B., & Song, K. H. (2017b). A role of pancreatic stellate cells in islet fibrosis and β-cell dysfunction in type 2 diabetes mellitus.

Biochemical and Biophysical Research Communications, *485*(2), 328–334. https://doi.org/10.1016/j.bbrc.2017.02.082

Ma, Y., Gao, M., & Liu, D. (2016). N-acetylcysteine Protects Mice from High Fat Diet-induced Metabolic Disorders. *Pharmaceutical Research*, *33*(8), 2033–2042. https://doi.org/10.1007/s11095-016-1941-1

Marie Kosiewicz, M., Richmond, J. M., Betts, M., Barcenilla hugobarcenilla, H., Barcenilla, H., Åkerman, L., … Casas, R. (2019). Mass Cytometry Identifies Distinct Subsets of Regulatory T Cells and Natural Killer Cells Associated With High Risk for Type 1 Diabetes. *Frontiers in Immunology | Www.Frontiersin.Org*, *1*, 982. https://doi.org/10.3389/fimmu.2019.00982

Marín-Peñalver, J. J., Martín-Timón, I., Sevillano-Collantes, C., & Del Cañizo-Gómez, F. J. (2016). Update on the treatment of type 2 diabetes mellitus. *World Journal of Diabetes*, *7*(17), 354–395. https://doi.org/10.4239/wjd.v7.i17.354

Masamune, A., Watanabe, T., Kikuta, K., & Shimosegawa, T. (2009). Roles of Pancreatic Stellate Cells in Pancreatic Inflammation and Fibrosis. *Clinical Gastroenterology and Hepatology*, *7*(11), S48–S54. https://doi.org/10.1016/J.CGH.2009.07.038

McAdam-Marx, C., Mukherjee, J., Bellows, B. K., Unni, S., Ye, X., Iloeje, U., & Brixner, D. I. (2014). Evaluation of the relationship between weight change and glycemic control after initiation of antidiabetic therapy in patients with type 2 diabetes using electronic medical record data. *Diabetes Research and Clinical Practice*, *103*(3), 402–411. https://doi.org/10.1016/j.diabres.2013.12.038

Mekada, K., Abe, K., Murakami, A., Nakamura, S., Nakata, H., Moriwaki, K., … Yoshiki, A. (2009). *Genetic Differences among C57BL/6 Substrains*. *Exp. Anim* (Vol. 58). Retrieved from http://jaxmice.jax.

Miki, A., Ricordi, C., Sakuma, Y., Yamamoto, T., Misawa, R., Mita, A., … Ichii, H. (2018). Divergent antioxidant capacity of human islet cell subsets: A potential cause of beta-cell vulnerability in diabetes and islet transplantation. *PLOS ONE*, *13*(5), e0196570. https://doi.org/10.1371/journal.pone.0196570

Mokhtari, V., Afsharian, P., Shahhoseini, M., Kalantar, S. M., & Moini, A. (2017). A review on various uses of N-acetyl cysteine. *Cell Journal*. Retrieved from https://www-ncbi-nlm-nih-gov.proxy1.lib.uwo.ca/pmc/articles/PMC5241507/pdf/Cell-J-19-11.pdf

Mosser, R. E., Maulis, M. F., Moullé, V. S., Dunn, J. C., Carboneau, B. A., Arasi, K., … Gannon, M. (2015). High-fat diet-induced β-cell proliferation occurs prior to insulin resistance in C57Bl/6J male mice. *American Journal of Physiology. Endocrinology and Metabolism*, *308*(7), E573-82. https://doi.org/10.1152/ajpendo.00460.2014

Nicholson, A., Reifsnyder, P. C., Malcolm, R. D., Lucas, C. A., MacGregor, G. R., Zhang, W., & Leiter, E. H. (2010). Diet-induced obesity in two C57BL/6 substrains with intact or mutant nicotinamide nucleotide transhydrogenase (Nnt) gene. *Obesity*, *18*(10), 1902–1905. https://doi.org/10.1038/oby.2009.477

Novelli, E. L. B., Santos, P. P., Assalin, H. B., Souza, G., Rocha, K., Ebaid, G. X., …

Fernandes, A. A. (2009). N-acetylcysteine in high-sucrose diet-induced obesity: Energy expenditure and metabolic shifting for cardiac health. *Pharmacological Research*, *59*(1), 74–79. https://doi.org/10.1016/j.phrs.2008.10.004

Pandol, S. J., & Edderkaoui, M. (2015). What are the macrophages and stellate cells doing in pancreatic adenocarcinoma? *Frontiers in Physiology*, *6*, 125. https://doi.org/10.3389/fphys.2015.00125

Pedersen, M., Tagliavini, A., & Henquin, J. C. (2019). Calcium signaling and secretory granule pool dynamics underlie biphasic insulin secretion and its amplification by glucose: Experiments and modeling. *American Journal of Physiology - Endocrinology and Metabolism*, *316*(3), E475–E486. https://doi.org/10.1152/ajpendo.00380.2018

Porter, A. G., & Jänicke, R. U. (1999). Emerging roles of caspase-3 in apoptosis. *Cell Death and Differentiation*. https://doi.org/10.1038/sj.cdd.4400476

Prentki, M., & Nolan, C. J. (2006a). Islet beta cell failure in type 2 diabetes. *The Journal of Clinical Investigation*, *116*(7), 1802–1812. https://doi.org/10.1172/JCI29103

Prentki, M., & Nolan, C. J. (2006b). Islet β cell failure in type 2 diabetes. *Journal of Clinical Investigation*. https://doi.org/10.1172/JCI29103

Rani, V., Deep, G., Singh, R. K., Palle, K., & Yadav, U. C. S. (2016). Oxidative stress and metabolic disorders: Pathogenesis and therapeutic strategies. *Life Sciences*. https://doi.org/10.1016/j.lfs.2016.02.002

Rendina-Ruedy, E., Hembree, K. D., Sasaki, A., Davis, M. R., Lightfoot, S. A., Clarke, S. L., … Biesalski, H. K. (2015). A Comparative Study of the Metabolic and Skeletal Response of C57BL/6J and C57BL/6N Mice in a Diet-Induced Model of Type 2 Diabetes. https://doi.org/10.1155/2015/758080

Rochette, L., Zeller, M., Cottin, Y., & Vergely, C. (2014). Diabetes, oxidative stress and therapeutic strategies. *Biochimica et Biophysica Acta - General Subjects*. https://doi.org/10.1016/j.bbagen.2014.05.017

Roma, L. P., M Oliveira, C. A., Carneiro, E. M., Albuquerque, G. G., Boschero, A. C., & A Souza, K. L. (2013). Redox Report Communications in Free Radical Research N-acetylcysteine protects pancreatic islet against glucocorticoid toxicity N-acetylcysteine protects pancreatic islet against glucocorticoid toxicity. https://doi.org/10.1179/1351000211Y.0000000006

Rossmeisl, M., Rim, J. S., Koza, R. A., & Kozak, L. P. (2003). Variation in type 2 diabetes - Related traits in mouse strains susceptible to diet-induced obesity. *Diabetes*, *52*(8), 1958–1966. https://doi.org/10.2337/diabetes.52.8.1958

Ryu, G. R., Lee, E., Chun, H.-J., Yoon, K.-H., Ko, S.-H., Ahn, Y.-B., & Song, K.-H. (2013). Oxidative stress plays a role in high glucose-induced activation of pancreatic stellate cells. *Biochemical and Biophysical Research Communications*, *439*(2), 258–263. https://doi.org/10.1016/j.bbrc.2013.08.046

Saito, R., Yamada, S., Yamamoto, Y., Kodera, T., Hara, A., Tanaka, Y., … Kojima, I. (2012). Conophylline Suppresses Pancreatic Stellate Cells and Improves Islet

Fibrosis in Goto-Kakizaki Rats. *Endocrine Society*. https://doi.org/10.1210/en.2011-1767

Sasson, A., Rachi, E., Sakhneny, L., Baer, D., Lisnyansky, M., Epshtein, A., & Landsman, L. (2016). Islet Pericytes Are Required for β-Cell Maturity. *Diabetes*, *65*(10), 3008–3014. https://doi.org/10.2337/db16-0365

Sekhar, R. V, McKay, S. V, Patel, S. G., Guthikonda, A. P., Reddy, V. T., Balasubramanyam, A., & Jahoor, F. (2011). Glutathione synthesis is diminished in patients with uncontrolled diabetes and restored by dietary supplementation with cysteine and glycine. *Diabetes Care*, *34*(1), 162–167. https://doi.org/10.2337/dc10-1006

Shen, F.-C., Weng, S.-W., Tsao, C.-F., Lin, H.-Y., Chang, C.-S., Lin, C.-Y., … Weng, W. (2019). Early intervention of N-acetylcysteine better improves insulin resistance in diet-induced obesity mice. https://doi.org/10.1080/10715762.2018.1447670

Sies, H. (2017). Hydrogen peroxide as a central redox signaling molecule in physiological oxidative stress: Oxidative eustress. *Redox Biology*, *11*, 613–619. https://doi.org/10.1016/j.redox.2016.12.035

Skovsø, S. (2014). Modeling type 2 diabetes in rats using high fat diet and streptozotocin. *Journal of Diabetes Investigation*, *5*(4), 349–358. https://doi.org/10.1111/jdi.12235

Springer-Verlag, @, Witschi, A., Reddy, S., Stofer, B., & Lauterburg, B. H. (1992). *The systemic availability of oral glutathione*. *Eur J Clin PharmacoI* (Vol. 43). Retrieved from https://journals-scholarsportal-info.proxy1.lib.uwo.ca/pdf/00316970/v43i0006/667_tsaoog.xml

Straub, S. G., & Sharp, G. W. G. (2002). Glucose-stimulated signaling pathways in biphasic insulin secretion. *Diabetes/Metabolism Research and Reviews*, *18*(6), 451–463. https://doi.org/10.1002/dmrr.329

Swisa, A., Glaser, B., & Dor, Y. (2017). Metabolic stress and compromised identity of pancreatic beta cells. *Frontiers in Genetics*. https://doi.org/10.3389/fgene.2017.00021

Szkudlinska, M. A., Von Frankenberg, A. D., & Utzschneider, K. M. (2016). The Antioxidant N-Acetylcysteine Does Not Improve Glucose Tolerance or β-Cell Function in Type 2 Diabetes HHS Public Access. *J Diabetes Complications*, *30*(4), 618–622. https://doi.org/10.1016/j.jdiacomp.2016.02.003

Tanaka, Y., Gleason, C. E., Oanh, P., Tran, T., Harmon, J. S., & Robertson, R. P. (1999). *Prevention of glucose toxicity in HIT-T15 cells and Zucker diabetic fatty rats by antioxidants (diabetesinsulin geneoxidative stressglucotoxicity)*. *Medical Sciences Communicated by Donald C. Malins* (Vol. 96). Retrieved from www.pnas.org.

Tanaka, Y., Oanh, P., Tran, T., Harmon, J., & Robertson, R. P. (2002). *A role for glutathione peroxidase in protecting pancreatic cells against oxidative stress in a model of glucose toxicity*. Retrieved from www.pnas.orgcgidoi10.1073pnas.192445199

Titchenell, P. M., Lazar, M. A., Birnbaum, M. J., Titchenell, P. M., Com, M. B., &

Birnbaum, M. J. (2017). Unraveling the Regulation of Hepatic Metabolism by Insulin. *Trends in Endocrinology & Metabolism*, *28*(7). https://doi.org/10.1016/j.tem.2017.03.003

Tome, M. E., Jaramillo, M. C., & Briehl, M. M. (2011). Hydrogen peroxide signaling is required for glucocorticoid-induced apoptosis in lymphoma cells. *Free Radical Biology & Medicine*, *51*(11), 2048–2059. https://doi.org/10.1016/j.freeradbiomed.2011.09.002

Tran, T., Parker, S. M., Leroy, E., Franklin, C. C., Kavanagh, T. J., Zhang, T., … Robertson, R. P. (2004). Adenoviral Overexpression of the Glutamylcysteine Ligase Catalytic Subunit Protects Pancreatic Islets against Oxidative Stress* Downloaded from. *THE JOURNAL OF BIOLOGICAL CHEMISTRY*, *279*(52), 53988–53993. https://doi.org/10.1074/jbc.M404809200

Tranberg, B., Hansen, A. K., & Lykkesfeldt, J. (2014). High-fat feeding increases hepatic vitamin C synthesis and its circulatory mobilization in mice. *European Journal of Nutrition*, *53*(6), 1441–1444. https://doi.org/10.1007/s00394-014-0694-z

Wang, R. N., Bouwens, L., & Klöppel, G. (1994). Beta-cell proliferation in normal and streptozotocin-treated newborn rats: site, dynamics and capacity. *Diabetologia*, *37*(11), 1088–1096. https://doi.org/10.1007/BF00418372

Wu, Fang, Y.-Z., Yang, S., Lupton, J. R., & Turner, N. D. (2004). Glutathione Metabolism and Its Implications for Health. *The Journal of Nutrition*, *134*(3), 489–492. https://doi.org/10.1093/jn/134.3.489

Wu, Y., Ding, Y., Tanaka, Y., & Zhang, W. (2014). Risk factors contributing to type 2 diabetes and recent advances in the treatment and prevention. *International Journal of Medical Sciences*, *11*(11), 1185–1200. https://doi.org/10.7150/ijms.10001

Xue, R., Jia, K., Wang, J., Yang, L., Wang, Y., & Gao, L. (2018). A Rising Star in Pancreatic Diseases: Pancreatic Stellate Cells. https://doi.org/10.3389/fphys.2018.00754

Yang, G., Li, C., Gong, Y., Fang, F., Tian, H., Li, J., & Cheng, X. (2016). Assessment of insulin resistance in subjects with normal glucose tolerance, hyperinsulinemia with normal blood glucose tolerance, impaired glucose tolerance, and newly diagnosed type 2 diabetes (prediabetes insulin resistance research). *Journal of Diabetes Research*. https://doi.org/10.1155/2016/9270768

Zang, G., Sandberg, M., Carlsson, P.-O., Welsh, N., Jansson, L., & Barbu, A. (2015a). Activated pancreatic stellate cells can impair pancreatic islet function in mice. *Upsala Journal of Medical Sciences*, *120*(3), 169–180. https://doi.org/10.3109/03009734.2015.1032453

Zang, G., Sandberg, M., Carlsson, P.-O., Welsh, N., Jansson, L., & Barbu, A. (2015b). Activated pancreatic stellate cells can impair pancreatic islet function in mice. *Upsala Journal of Medical Sciences*, *120*(3), 169–180. https://doi.org/10.3109/03009734.2015.1032453

Zha, M., Li, F., Xu, W., Chen, B., & Sun, Z. (2014). Isolation and characterization of islet stellate cells in rat. *Islets*, *6*(2), e28701. https://doi.org/10.4161/isl.28701

Zhang, Kim, D. H., Xiao, X., Lee, S., Gong, Z., Muzumdar, R., … Dong, H. H. (2016). Foxo1 plays an important role in regulating β-cell compensation for insulin resistance in male mice. *Endocrinology*, *157*(3), 1055–1070. https://doi.org/10.1210/en.2015-1852

Zhang, X., Bao, Y., Ke, L., & Yu, Y. (2010). Elevated circulating free fatty acids levels causing pancreatic islet cell dysfunction through oxidative stress. https://doi.org/10.3275/6621

Appendices

Appendix A: 2017-093 Animal Use Protocol (AUP)

Western

2017-093:2:

AUP Number: 2017-093
AUP Title: Studies of the functional role of pancreatic stellate cells (PaSCs) in duct-ligation and HFD-induced diabetic pancreas.
Yearly Renewal Date: 02/01/2020

The YEARLY RENEWAL to Animal Use Protocol (AUP) 2017-093 has been approved by the Animal Care Committee (ACC), and will be approved through to the above review date.

Please at this time review your AUP with your research team to ensure full understanding by everyone listed within this AUP.

As per your declaration within this approved AUP, you are obligated to ensure that:

1) Animals used in this research project will be cared for in alignment with:
   a) Western's Senate MAPPs 7.12, 7.10, and 7.15
   http://www.uwo.ca/univsec/policies_procedures/research.html
   b) University Council on Animal Care Policies and related Animal Care Committee procedures
   http://uwo.ca/research/services/animalethics/animal_care_and_use_policies.html
2) As per UCAC's Animal Use Protocols Policy,
   a) this AUP accurately represents intended animal use;
   b) external approvals associated with this AUP, including permits and scientific/departmental peer approvals, are complete and accurate;
   c) any divergence from this AUP will not be undertaken until the related Protocol Modification is approved by the ACC; and
   d) AUP form submissions - Annual Protocol Renewals and Full AUP Renewals - will be submitted and attended to within timeframes outlined by the ACC. http://uwo.ca/research/services/animalethics/animal_use_protocols.html
3) As per MAPP 7.10 all individuals listed within this AUP as having any hands-on animal contact will
   a) be made familiar with and have direct access to this AUP;
   b) complete all required CCAC mandatory training (training@uwo.ca); and
   c) be overseen by me to ensure appropriate care and use of animals.
4) As per MAPP 7.15,
   a) Practice will align with approved AUP elements;
   b) Unrestricted access to all animal areas will be given to ACVS Veterinarians and ACC Leaders;
   c) UCAC policies and related ACC procedures will be followed, including but not limited to:
      i) Research Animal Procurement
      ii) Animal Care and Use Records
      iii) Sick Animal Response
      iv) Continuing Care Visits
5) As per institutional OH&S policies, all individuals listed within this AUP who will be using or potentially exposed to hazardous materials will have completed in advance the appropriate institutional OH&S training, facility-level training, and reviewed related (M)SDS Sheets, http://www.uwo.ca/hr/learning/required/index.html

Submitted by: Copeman, Laura
on behalf of the Animal Care Committee
University Council on Animal Care

The University of Western Ontario
Animal Care Committee / University Council on Animal Care
London, Ontario Canada N6A 5C1
519-661-2111 x 88792 Fax 519-661-2028
auspc@uwo.caï¿½ http://www.uwo.ca/research/services/animalethics/index.html

Appendix B: Biosafety Approval Form

BIOSAFETY PERMIT

LAWSON
HEALTH RESEARCH INSTITUTE

Dear Dr. Wang

Your biosafety approval number is **BSP-LHSC-0019**. This number is a requirement for your research grants, purchasing of biohazardous materials and Level 2 inspections. Please use this number on all correspondence with the Biosafety Officer (BSO).

This permit expires on **April 4, 2020**.

Research Grants

Your study's LBAPP number is required for any research grants involving biohazards. Please provide this number to Research Services when requested.

Purchasing Materials

Your LBAPP number must be included on purchase orders for all Risk Group 1 and Risk Group 2 pathogens and toxins. Please include your name as the Primary Investigator (PI) and your biosafety approval number on all purchase order through HMMS or on all University of Western Ontario purchases.

Annual Inspections

Your Containment Level 2 laboratory will be inspected every year by the BSO and Lawson Safety Analyst.

This permit allows you to work with Risk Group 1 and Risk Group 2 biohazardous agents.

To maintain your Biosafety Permit, you will need to:

- Have a complete, up to date Biohazardous Agents inventory;
- Ensure that the employees, students and researchers working in your laboratory are trained in Biosafety;
- Ensure that your laboratory follows the requirements of the Lawson Biosafety Manual and mitigation strategies on your Biosafety / Biosecurity Risk Assessment; and
- Follow the guidance of the BSO and Lawson Safety Analyst on laboratory safety.

Please let me know if you have questions or comments.

Regards,

Charis Johnson-Antaran, MSc
Biosafety Officer
Lawson Health Research Institute

The Research Institute of London Health Sciences Centre and St. Joseph's Health Care London.

London Health Sciences Centre St JOSEPH'S Western

Appendix C: Picrosirius red staining of iNAC liver samples

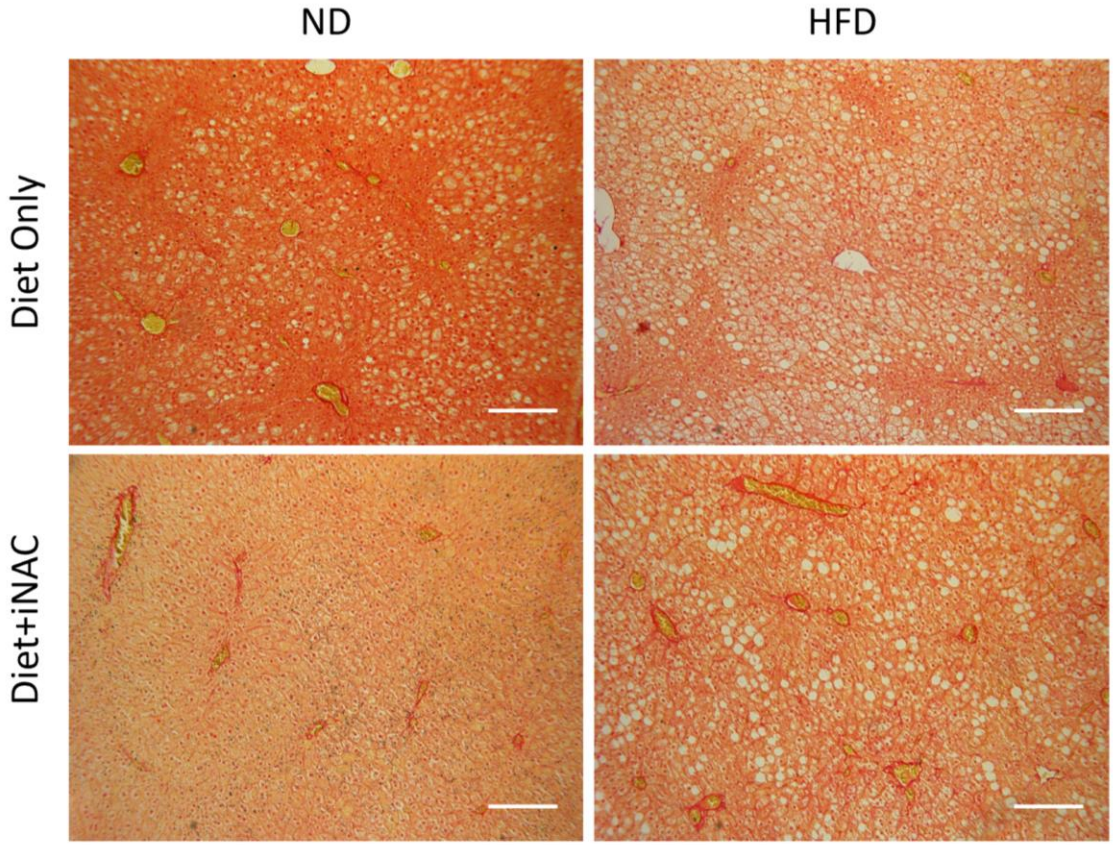

22-week ND, HFD, ND+iNAC, and HFD+iNAC treated samples were stained for picrosirius red to detect fibrosis and steatosis. Scale bar, 50μm.

Appendix D: IF Staining Controls for αSMA

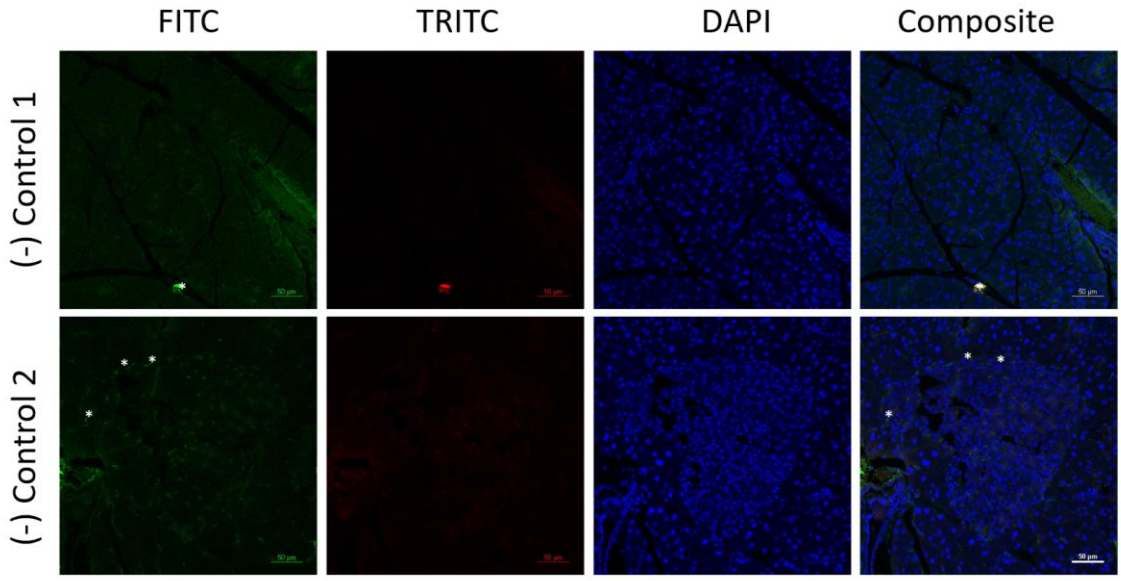

4% PFA fixed and paraffin embedded adult mouse pancreatic tissue was stained for: anti-αSMA antibody only in (-) control 1 or FITC-conjugated anti-mouse and TRITC-conjugated anti-rabbit IgG only in (-) control 2. Nuclei were stained for DAPI. Scale bar, 50μm. Asterisks indicate non-specific staining of blood cells, also demonstrated by overlap in FITC and TRITC in composite images.

Curriculum Vitae

Wallace, Madison

Post-Secondary Education

Master of Science Candidate: Pathology and Laboratory Medicine

Western University, London, ON

May 2017-Present

Bachelor of Science: Biology

Ohio Valley University, Vienna, WV

August 2012-May 2016

Honors/ Awards

Scholarships

2017-2019 **Western Graduate Research Scholarship**
Western University
1500/Term

2013-2016 **Softball Scholarship**
Ohio Valley University

10, 000/Year

2012-2016 **Academic Scholarship**
Ohio Valley University

5, 000/Year

2012-2013 **Volleyball Scholarship**
Ohio Valley University

10, 000/Year

Awards/Recognition

May 2016 **Graduated Summa Cum Laude**, Ohio Valley University, Distinction

May 2016 **Who's Who Among Students in American Universities and Colleges**, Who's Who Among Students in American Universities and Colleges, Distinction

2012-2016 **Honor Roll,** Ohio Valley University, Distinction

2014-2015 **GMAC All-Academic Team,** GMAC athletic conference, Distinction

Abstracts and Presentations

April 2019 **London Health Research Day**

March 2017- **Pathology and Laboratory Medicine Research Day**
March 2019

Publications

Wu M, Li XJ, Wallace M, Lin X. (2018). Autologous Transplantation of the Neurosensory Retina for Refractory Macular Holes. Journal of Clinical and Experimental Ophthalmology. 9(4): 739.

Graduate Teaching Assistantships

Sept 2017-
April 2019 **Graduate Teaching Assistant**, MedSci3900 IMS Laboratory, UWO
Role: Instruct 3rd year IMS students during introductory laboratory techniques (cell culture, cloning, ELISA, IF staining) as well as marking coursework and proctoring exams.